Localizing the Strange Chaotic Attractors of Multiparameter Nonlinear Dynamical Systems using a Geometric Approach involving Competitive Modes: A Master's Thesis

H.A.J. Reijm

Delft University of Technology

h.a.j.reijm@student.tudelft.nl

UNDER THE SUPERVISION OF

Prof. Cornelis Vuik

Delft University of Technology

c.vuik@tudelft.nl

Dr. Sudipto "Roy" Choudhury

University of Central Florida

sudipto.choudhury@ucf.edu

April 26, 2019

Contents

I. Introduction

Dynamical systems are a essential part of the modern mathematical and physical community. They're popularity can be attested to in almost all aspects of science. As an example, consider the system of differential equations describing the motion of an object under the influence of some constant downward acceleration.

$$\begin{cases} \dot{a}(t) = 0 \\ \dot{v}(t) = a(t) \\ \dot{x}(t) = v(t) \end{cases}$$

Here, $x(t)$ describes the vertical position of the object, $v(t)$ describes its velocity, and $a(t)$ describes its acceleration, all with respect to time t. This differential equation can easy be solved as follows.

$$\begin{cases} a(t) = a(0) \\ v(t) = a(0)t + v(0) \\ x(t) = \frac{1}{2}a(0)t^2 + v(0)t + x(0) \end{cases} \tag{1}$$

This system of solutions is referred to as a dynamical system. Here we see the purpose of dynamical systems: describing the solutions of differential equations. We state this more formally with the following definition.

Definition I.1. ***Dynamical System***
Say we have a continuous system of differential equations $\dot{\mathbf{x}} = \mathbf{F}(\mathbf{x}, t)$ *with* $\mathbf{F} : S \times \mathbb{R} \to S$*, where* S *is some open subset of* $\mathbb{R}^n$*.*
The dynamical system $\delta : S \times \mathbb{R} \to S$ *is a continuously differentiable mapping that defines the solution curve of our system of differential equations that passes through the point* $\mathbf{x}_0 \in S$ *at* $t = 0$ *[15][23].*

Some dynamical systems are much more complicated than Equation (1) and require numerical integration techniques in order to be approximated (direct solutions are often impossible to find). A particularly famous example of such a dynamical system is that of the Lorenz system [19].

$$\begin{cases} \dot{x} = \sigma(y - x) \\ \dot{y} = x(\rho - z) - y \\ \dot{z} = xy - \beta z \end{cases} \tag{2}$$

Here, σ, ρ, and $\beta \in \mathbb{R}$, and x, y, z are real functions of $t \in \mathbb{R}$.

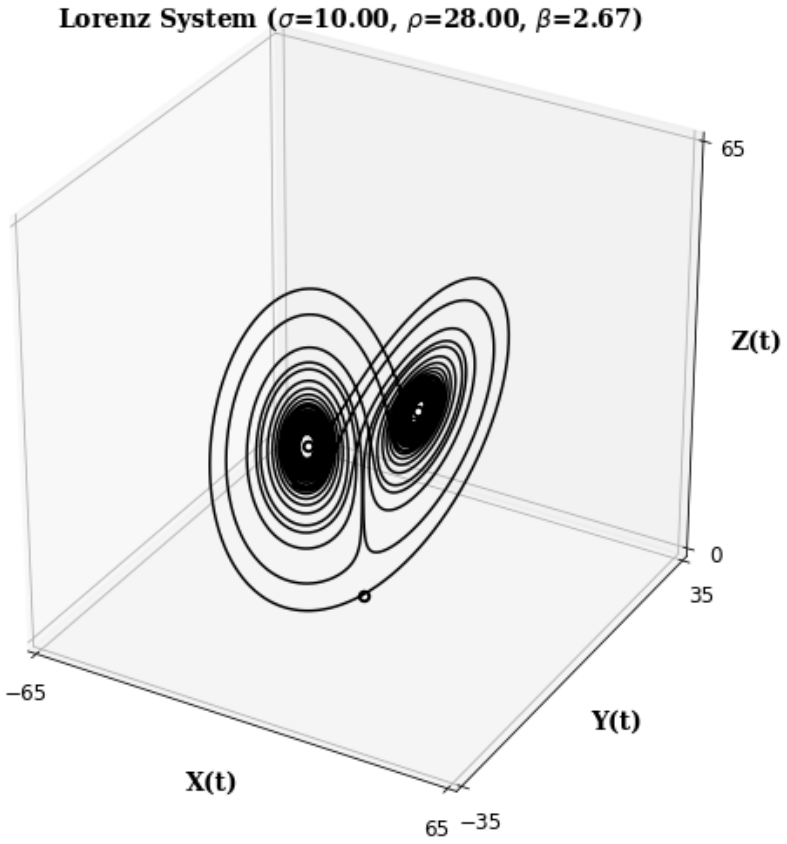

Figure 1: *The Lorenz attractor, where $\sigma = 10$, $\rho = 28$, and $\beta = 8/3$. Here, we generate this attractor from solution curves originating very near the origin, which is an equilibrium point of this system (an equilibrium point of a system of differential equations $\dot{\mathbf{x}} = \mathbf{F}(\mathbf{x}, t)$ is a point $\mathbf{x}_e$ in the phase space where $\dot{\mathbf{x}}_e = \mathbf{0}$).*

We can numerically approximate the dynamical system to the Lorenz system using an explicit Runge Kutta method. Choosing a specific set of parameters and initial conditions, we plot approximations to specific solution curves in the x,y,z-graph (called a phase space) in Figure 1. As a result, we see a very curious structure forming in the phase space: it seems that the solution curves we plotted eventually converge to some bounded set in the phase space, something that resembles the wings of a butterfly. This set is called the Lorenz Attractor, a classic example of the more general concept of a strange attractor [15].

Strange attractors, because of their complicated structures and ability to describe steady-state situations, are a topic of great interest in the modern dynamical systems

community. Being able to efficiently and easily visualize them would be a significant step forward in terms of mathematical research. In this document, we will be exploring the properties of strange attractors, as well as investigating the current methods used to visualize them. We will then be analyzing a new method of visualization, explaining its inner workings, applying it to well-known dynamical systems, and comparing it to the visualization methods currently available.

II. Strange Attractors in Dynamical Systems

In Section I, we loosely explained some basic concepts concerning dynamical systems but refrained from concretely defining them. Let us first rectify this.

Definition II.1. ***Attracting Set***
Lets say we have the dynamical system $\delta : S \times \mathbb{R} \to S$ of a system of differential equations. A closed, invariant set $A \subseteq S$ is called an attracting set of our system of differential equations if there exists some neighborhood N of A such that any solution trajectory $\delta(\mathbf{x}, \cdot)$ with $\mathbf{x} \in N$ has a $t_A \geq 0$ so that $\delta(\mathbf{x}, t) \in A$ for all $t \geq t_A$ [15]. The maximal neighborhood N_{max} of A where this is the case is called the basin of attraction of A.

Definition II.2. ***Attractor***
Lets say we have the dynamical system $\delta : S \times \mathbb{R} \to S$ of a system of differential equations. Suppose A is an attracting set of our system of differential equations. The set A is an attractor if it contains a dense orbit; that is, there exists a trajectory that passes through or comes infinitely close to every point in A. This ensures that A is not the union of two or more distinct attracting sets [15][21].

Attractors are not an uncommon sight in dynamical systems: stable equilibrium points, stable limit cycles, and stable limit tori are all examples of attractors that can occur in a dynamical system. However, defining whether an attractor is strange or not takes some more effort, and it all has to do with the concept of dimension.

Lets say we have a nonempty set B in $\mathbb{R}^n$. The topological dimension of B is simply the formal name for the well-known, everyday concept of dimensionality. According to topological dimensionality, a point is 0-dimensional, a line is 1-dimensional, a plane is 2-dimensional, and so on. Notice that the topological dimension of B is always an integer value greater or equal to 0, and no greater than n [13].

We must define another concept of dimensionality before we can proceed. Suppose we have the set B defined as before. We define the s-dimensional Hausdorff measure of B as follows [7]:

$$\mathcal{H}^s(B) = \lim_{\varepsilon \to 0} \inf \left\{ \sum_{i=1}^{\infty} |C_i|^s : \ \{C_i\} \text{ is a } \varepsilon\text{-cover of } B \right\}$$

Here, a ε-cover of B is a countable set $\{C_i\}$ so that $\sup\{|x - y| : x, y \in C_i\} \leq \varepsilon \ \forall i$ and $B \subseteq \bigcup_{i=1}^{\infty} C_i$. Using this measure, we can define the Hausdorff dimension (or Hausdorff-Besicovitch dimension) of B as follows [7]:

$$dim_{\mathcal{H}}(B) = \inf\{s \geq 0 : \mathcal{H}^s(B) = 0\} \tag{3}$$

Now that we have defined the concepts of topological and Hausdorff dimensionality, we can move on to the defining of a fractal, which are essential structures in strange attractors.

Definition II.3. ***Fractal***
Say we have a nonempty set B in $\mathbb{R}^n$. The set B is a fractal if the Hausdorff dimension of B is strictly greater than the topological dimension of B [13]. Often, this is described as self-similarity: the fractal is constructed of parts that in turn resemble (not necessarily copy) the whole structure [7].

Finally, we can define a strange attractor very simply.

Definition II.4. ***Strange Attractor***
Lets say we have the dynamical system $\delta : S \times \mathbb{R} \to S$ of a system of differential equations. Suppose A is an attractor of our set of differential equations. The set A is a strange attractor if its attracting set is fractal in nature. In layman's terms, this means that A has a much more complicated geometric structure than, for example, an equilibrium point, a limit cycle, or limit torus [2][21].

We can further classify strange attractors in two categories: self-excited and hidden. However, in order to formally define these two categories, we must first provide a few more definitions.

Definition II.5. ***Equilibrium Point***
Lets say we have the system of differential equations $\dot{\mathbf{x}} = \mathbf{F}(\mathbf{x})$. An equilibrium point $\mathbf{x}_e$ of this system is a point in the phase space where $\mathbf{F}(\mathbf{x}_e) = \mathbf{0}$. In order words, the equilibrium point is invariant under the corresponding dynamical system. For our purposes, we require that an equilibrium point must be distinct, i.e. there exists a nonempty neighborhood around (but not including) $\mathbf{x}_e$ such that all points in this neighborhood are not equilibrium points [15].

Definition II.6. ***Manifolds of Equilibrium Points***
Lets say we have the dynamical system $\delta : S \times \mathbb{R} \to S$ of a system of differential equations that contains equilibrium point $\mathbf{x}_e$. A manifold $\mathcal{W}(\mathbf{x}_e)$ is a set of points in the phase space whereby either:

- $\lim_{t\to\infty} \delta(\mathbf{x}, t) = \mathbf{x}_e$ *for all* $\mathbf{x}$ *in* $\mathcal{W}(\mathbf{x}_e)$*, in which case the manifold is called a stable manifold* $\mathcal{W}^+(\mathbf{x}_e)$ *[2].*
- $\lim_{t\to-\infty} \delta(\mathbf{x}, t) = \mathbf{x}_e$ *for all* $\mathbf{x}$ *in* $\mathcal{W}(\mathbf{x}_e)$*, in which case the manifold is called an unstable manifold* $\mathcal{W}^-(\mathbf{x}_e)$ *[2].*

We can now define self-excited and hidden strange attractors.

Definition II.7. ***Classification of Strange Attractors***
Lets say we have a system of differential equations that contains equilibrium points. Suppose A is a strange attractor, then

- *A is self-excited if its basin of attraction contains at least one equilibrium point [11].*
- *A is hidden if its basin of attraction contains no equilibrium points [11].*

Per definition, self-excited strange attractors can be easily visualized by simply plotting the unstable manifolds of the equilibrium points, which are usually easy to find. At least one of the unstable manifolds will flow into the strange attractor and, given enough time, will show how the attractor behaves. On the other hand, finding hidden attractors is much more difficult since they can be located anywhere and are not accessible through the equilibrium points. Much more work and time is required to investigate if a hidden attractor is even present in the dynamical system, let alone how it is structured and where it is located. Currently, research is being done on how to locate hidden attractors more easily [11][10][12].

We present a few examples of strange attractors in the following subsection, all of which are self-excited attractors and thus easy to visualize.

i. Examples of Strange Attractors

i.1 Lorenz Attractor

As we have seen before in Section I, the Lorenz system is one of the most famous dynamical systems that can contain a strange attractor. For the reader's convenience, we again give the Lorenz system below [6][19].

$$\begin{cases} \dot{x} = \sigma(y - x) \\ \dot{y} = x(\rho - z) - y \\ \dot{z} = xy - \beta z \end{cases} \tag{4}$$

Here, σ, ρ, and β are all real valued parameters.

The first thing we want to do is present a lemma about the symmetrical nature of the Lorenz system.

Lemma II.1 (**Symmetry of the Lorenz System**)**.** *The Lorenz system is symmetric under the transformation* $(x, y, z) \to (-x, -y, z)$ *[15].*

Proof. The proving this lemma is extremely simple and can be done using the following equivalent statements.

$$\begin{aligned} \dot{x} = \sigma(y - x) &\equiv -\dot{x} = \sigma((-y) - (-x)) \\ \dot{y} = x(\rho - z) - y &\equiv -\dot{y} = (-x)(\rho - z) - (-y) \\ \dot{z} = xy - \beta z &\equiv \dot{z} = (-x)(-y) - \beta z \end{aligned}$$

□

This means that if one structure appears in the $+x, +y$-plane, then that same structure will appear in the $-x, -y$-plane. This is also true for any equilibrium points that the Lorenz system might have.

Speaking of equilibrium points, the Lorenz system, under very weak conditions, has the following equilibrium points.

Lemma II.2 (**Equilibrium Points of the Lorenz System**). *The equilibrium points* $\{(x_e, y_e, z_e)\}$ *of the Lorenz system given in Equation* (4) *with* $\beta \neq 0$ *are* $(0, 0, 0)$ *and* $(\pm\sqrt{\beta(\rho - 1)}, \pm\sqrt{\beta(\rho - 1)}, \rho - 1)$.

Proof. In the first equation, $\dot{x}_e = \sigma(y_e - x_e) = 0$, meaning that $x_e = y_e$.
In the second equation, $\dot{y}_e = x_e(\rho - z_e) - y_e = 0$, meaning that $y_e = x_e(\rho - z_e)$.
In the third equation, $\dot{z}_e = x_e y_e - \beta z_e = 0$, meaning that $\beta z_e = x_e y_e$.

Combining these three equations, $\beta y_e = y_e(\beta\rho - y_e^2)$, meaning that either $y_e = 0$ or $y_e = \pm\sqrt{\beta(\rho - 1)}$.
Thus, any equilibrium point of the Lorenz system where $\beta \neq 0$ must be either $(0, 0, 0)$ or $(\pm\sqrt{\beta(\rho - 1)}, \pm\sqrt{\beta(\rho - 1)}, \rho - 1)$. If $\beta = 0$, then the only equilibrium point of the system is the origin. □

Of course, this means that two of the equilibrium points of the Lorenz system do not exist in the real phase space unless $\beta > 0$ and $\rho > 1$. Because of this, we will indeed assume from now on that $\beta > 0$ and $\rho > 1$.

The Lorenz Attractor is constructed around the nonzero equilibrium points of the Lorenz system, spreading out like twisted butterfly wings. One of the easiest ways of visualizing this attractor is setting the parameter $\sigma = 10$, $\beta = 28$, and $\rho = 28$; indeed, these are the values that Lorenz himself used when he was first studying this system [6][19]. Figure 2 gives a visual representation of the Lorenz Attractor, using these parameter values.

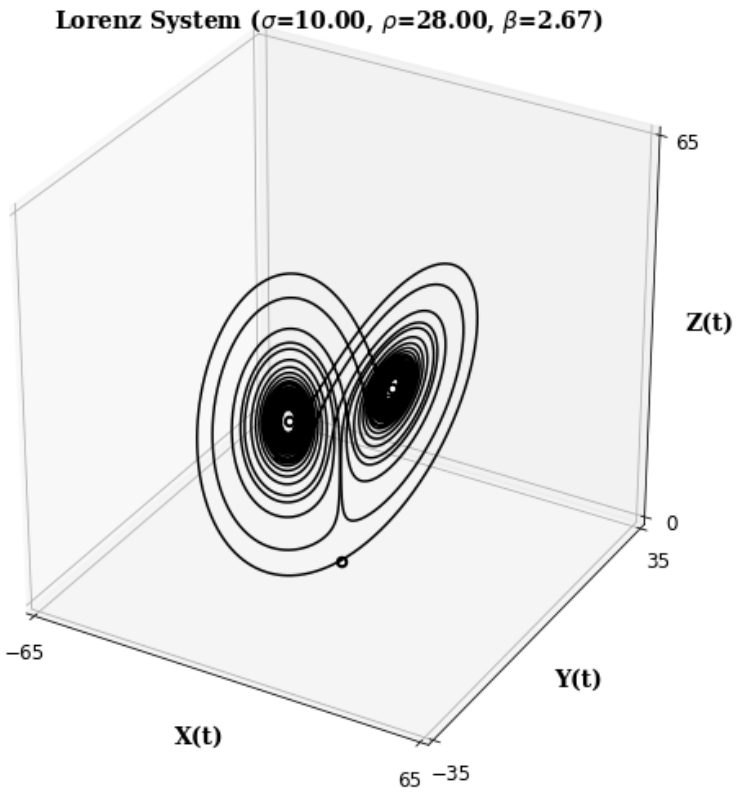

Figure 2: *The Lorenz Attractor, developed from the unstable manifolds of the origin, where* $\sigma = 10$*,* $\rho = 28$*, and* $\beta = 8/3$*.*

As one can see, the attractor per definition is invariant under the dynamical system: a trajectory inside the attractor will forever remain inside it. But it is the shape of the attractor that makes it strange. The Lorenz Attractor's structure is much more complicated that a simple attracting point or limit cycle; since the Lorenz Attractor was concretely proven to be a strange attractor in 2002, it has been confirmed that it is also indeed fractal in nature [22].

i.2 Chua Attractor

Chua Attractor occurs in a system of differential equations describing the current and voltage flowing through a simple electronic circuit consisting of two capacitors, one inductor, one nonlinear resistor, and a Chua diode [18]. The system was named after its founder Leon Chua, who introduced the system in the mid 1980's [14].

We will simply treat the Chua system as a mathematical system without paying too much attention to the physical interpretation of it. For this reason, we will be

working with a simplified version of the system, one which still exhibits the strange attractor we are looking for.

$$\begin{cases} \dot{x} = \alpha(y - x - f(x)) \\ \dot{y} = x - y + z \\ \dot{z} = -\beta y \end{cases} \tag{5}$$

Here, f is a nonlinear function that describes the change in resistance versus current in the Chua diode [18]. Mathematically, multiple sources of literature simply define the function as follows [14][18][11][10][12].

$$\begin{aligned} f(x) &= m_1 x + \frac{1}{2}(m_0 - m_1)(|x+1| - |x-1|) \\ &= \begin{cases} m_1 x + (m_1 - m_0) & x \in (-\infty, -1) \\ m_0 x & x \in [-1, 1] \\ m_1 x + (m_0 - m_1) & x \in (1, \infty) \end{cases} \end{aligned} \tag{6}$$

Now, we define the system's equilibrium points.

Lemma II.3 (**Equilibrium Points of the Chua System**). *The equilibrium points* $\{(x_e, y_e, z_e)\}$ *of the Chua system given in Equation* (5) *with nonlinearity function* f *defined in Equation* (6) *are*

$$\begin{gathered} (0,0,0) \text{ if } m_0 \neq 0 \\ \left(\frac{m_1 - m_0}{m_1 + 1}, 0, \frac{m_0 - m_1}{m_1 + 1}\right) \text{ if } (m_0 + 1)(m_1 + 1) < 0 \\ \left(\frac{m_0 - m_1}{m_1 + 1}, 0, \frac{m_1 - m_0}{m_1 + 1}\right) \text{ if } (m_0 + 1)(m_1 + 1) < 0 \end{gathered}$$

Proof. In the first equation, $\dot{x}_e = \alpha(y_e - x_e - f(x_e)) = 0$, meaning that $y_e = x_e + f(x_e)$.
In the second equation, $\dot{y}_e = x_e - y_e + z_e = 0$, meaning that $y_e = x_e + z_e$.
In the third equation, $\dot{z}_e = -\beta y_e = 0$, meaning that $y_e = 0$.

Combining these three equations, we immediately see that any equilibrium point of the Chua system is $(x_e, 0, -x_e)$ where $x_e + f(x_e) = 0$. Therefore, it is crucial to calculate x_e.

We mustfirst prove that the function f as defined in Equation (6) is an odd function; that is, $f(x) = -f(-x)$.

$$
\begin{aligned}
-f(-x) &= \begin{cases} -m_1(-x) - (m_1 - m_0) & -x \in (-\infty, -1) \\ -m_0(-x) & -x \in [-1, 1] \\ -m_1(-x) - (m_0 - m_1) & -x \in (1, \infty) \end{cases} \\
&= \begin{cases} m_1 x + (m_0 - m_1) & x \in (1, \infty) \\ m_0 x & x \in [-1, 1] \\ m_1 x + (m_1 - m_0) & x \in (-\infty, -1) \end{cases} \\
&= f(x)
\end{aligned}
$$

In this case, we can keep focus primarily on positive values of x. If there exists some intersect point x_e so that $x_e + f(x_e) = 0$, then $-x_e + f(-x_e) = 0$.

Furthermore, we only consider x_e to be a viable answer to the equation $x_e + f(x_e) = 0$ if there exists some open neighborhood in $\mathbb{R}$ around x_e that does not contain any other solution to the equation. This is in order to ensure that each resulting equilibrium point is its own individual, independent point in the phase space.

Say $x \in [0, 1]$.
Then $f(x) = m_0 x$. It is trivial to conclude that if $m0 \neq -1$, then $x_e + f(x_e) = 0$ if and only if $x_e = 0$. If $m0 = -1$, then x_e can be any value in $[0, 1]$. Thus, we do not consider the equation $x_e + f(x_e) = 0$ to have any viable solutions on $[0, 1]$ when $m0 = -1$.

Say $x \in (1, \infty)$.
Then $f(x) = m_1 x + (m_0 - m_1)$. Then $x_e + f(x_e) = 0$ for $x_e = (m_1 - m_0)/(m_1 + 1)$. The question is whether this value falls in the range $(1, \infty)$.

For ease of analysis, let us define a new function $g : \mathbb{R}^2 \to \mathbb{R}$, defined as $g(m_0, m_1) = (m_1 - m_0)/(m_1 + 1) = x_e$. The function g is almost everywhere differentiable, with the exception being when $m_1 = -1$.

$$
\begin{aligned}
\frac{\partial g}{\partial m_0} &= \frac{-1}{m_1 + 1} \\
\frac{\partial g}{\partial m_1} &= \frac{m_0 + 1}{(m_1 + 1)^2}
\end{aligned}
$$

Assume $m_0 < -1$.
Then $\partial g / \partial m_1 < 0$ for all $m_1 \in \mathbb{R} \backslash \{-1\}$. Also notice that $\lim_{m_1 \to \pm\infty} g = 1$. Thus, we can conclude that for $m_1 \in (-\infty, -1)$, the function g always takes on a value less than 1; in the same way for $m_1 \in (-1, \infty)$, the function g always takes on a value

greater than 1.

Since $g(m_0, m_1) = x_e$ and since we require $x_e \in (1, \infty)$, we can conclude that for $m_1 < -1$, the intersect point x_e does not exist. When $m_1 > -1$, then the intersect point is defined as $x_e = (m_1 - m_0)/(m_1 + 1) \in (1, \infty)$. If $m_1 = -1$, we can then immediately see that if $x_e + f(x_e) = 0$, then $m_0 = -1$. However, because $m_0 < -1$, the intersect point x_e cannot exist.

Assume $m_0 > -1$.
Then $\partial g/\partial m_1 > 0$ for all $m_1 \in \mathbb{R}\backslash\{-1\}$. Also notice that $\lim_{m_1 \to \pm\infty} g = 1$. Thus, we can conclude that for $m_1 \in (-\infty, -1)$, the function g always takes on a value greater than 1; in the same way for $m_1 \in (-1, \infty)$, the function g always takes on a value less than 1.

Since $g(m_0, m_1) = x_e$ and since we require that $x_e \in (1, \infty)$, we can conclude that for $m_1 > -1$, the intersect point x_e does not exist. When $m_1 < -1$, then the intersect point is defined as $x_e = (m_1 - m_0)/(m_1 + 1) \in (1, \infty)$. If $m_1 = -1$, we can then immediately see that if $x_e + f(x_e) = 0$, then $m_0 = -1$. However, because $m_0 > -1$, the intersect point x_e cannot exist.

Assume $m_0 = -1$
Then $x_e + f(x_e) = 0 \Leftrightarrow (m_1 + 1)x_e = (m_1 + 1)$. From this we can must conclude that $m_1 = -1$ since $x_e > 1$. However, if $m_1 = -1$, then x_e can be any value in $(1, \infty)$. Thus, we do not consider the equation $x_e + f(x_e) = 0$ to have any viable solutions on $(1, \infty)$ if $m_0 = -1$.

Therefore, the only viable solution for $x_e \in (1, \infty)$ is

$$x_e = \frac{m_1 - m_0}{m_1 + 1} \text{ if } (m_0 + 1)(m_1 + 1) < 0$$

However, we proved previously that that the function $f(x)$ is odd. Therefore, we can immediately conclude that the only viable solution for $x_e \in (-\infty, -1)$ is

$$x_e = \frac{m_0 - m_1}{m_1 + 1} \text{ if } (m_0 + 1)(m_1 + 1) < 0$$

In conclusion, the only equilibrium points of the Chua system are

$$(0, 0, 0) \text{ if } m_0 \neq 0$$
$$\left(\frac{m_1 - m_0}{m_1 + 1}, 0, \frac{m_0 - m_1}{m_1 + 1}\right) \text{ if } (m_0 + 1)(m_1 + 1) < 0$$
$$\left(\frac{m_0 - m_1}{m_1 + 1}, 0, \frac{m_1 - m_0}{m_1 + 1}\right) \text{ if } (m_0 + 1)(m_1 + 1) < 0$$

□

The Chua Attractor twists around all three equilibrium points when they exist, sometimes generating a structure that most people describe as the "double scroll" [18]. We visualize this attractor by choosing an appropriate set of parameters and plot the unstable manifolds of the origin. Given enough time, they give an accurate representation of Chua's "double scroll", as shown in Figure 3.

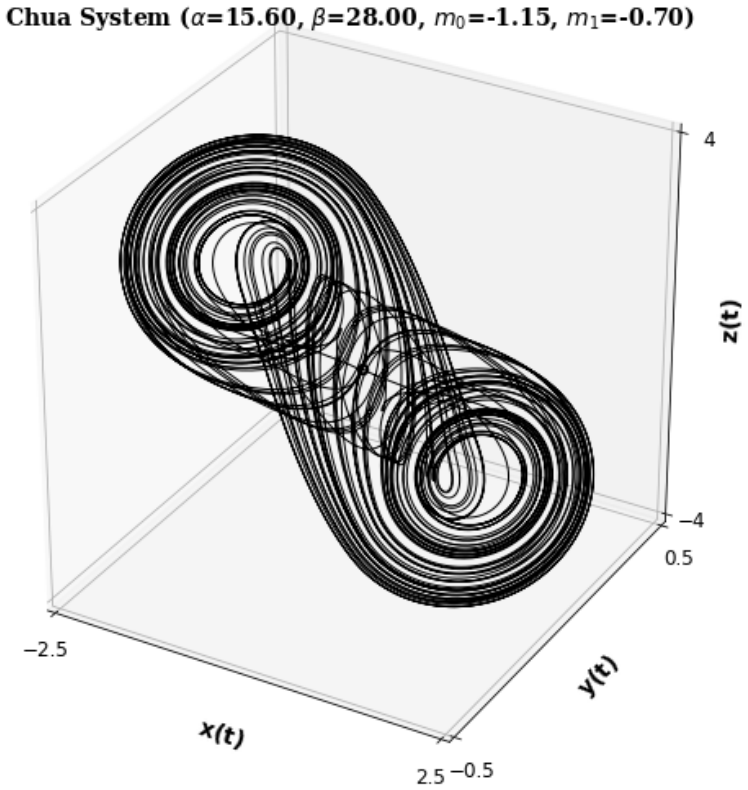

Figure 3: *The Chua Attractor, developed from the unstable manifolds of the origin, where* $\alpha = 15.6$*,* $\beta = 28$*,* $m_0 = -1.15$ *and* $m_1 = -0.7$ *[18]. The strange attractor revolves around all three equilibrium points, which in this case are (0, 0, 0), (1.5, 0, -1.5), and (-1.5, 0, 1.5).*

Again, we can see from this complicated invariant structure that this is indeed a strange attractor.

i.3 Rössler Attractor

The Rössler Attractor was first described by O. Rössler in 1976 as a play model for many physical and chemical phenomenon, including the Lorenz system [16]. The

Rössler system of equations is simply given as

$$\begin{cases} \dot{x} = -(y+z) \\ \dot{y} = x + \alpha y \\ \dot{z} = \beta + z(x-\gamma) \end{cases} \tag{7}$$

Here, parameters α, β, and γ are real-valued parameters. The equilibrium points of this system are of particular interest and as such are defined in the following lemma.

Lemma II.4 (**Equilibrium Points of the Rössler System**). *The equilibrium points* $\{(x_e, y_e, z_e)\}$ *of the Rössler system given by Equation* (7) *with* $\alpha \neq 0$ *is given by*

$$\left(\frac{\gamma \pm \sqrt{\gamma^2 - 4\alpha\beta}}{2}, \frac{-\gamma \mp \sqrt{\gamma^2 - 4\alpha\beta}}{2\alpha}, \frac{\gamma \pm \sqrt{\gamma^2 - 4\alpha\beta}}{2\alpha} \right)$$

Proof. In the first equation, $\dot{x}_e = -(y_e + z_e) = 0$, meaning that $y_e = -z_e$.
In the second equation, $\dot{y}_e = x_e + \alpha y_e = 0$, meaning that $x_e = -\alpha y_e$.
In the third equation, $\dot{z}_e = \beta + z_e(x_e - \gamma) = 0$, meaning that $z_e x_e - \gamma z_e + \beta = 0$.

Combining these three equations, $\alpha z_e^2 - \gamma z_e + \beta = 0$,
meaning that $z_e = (\gamma \pm \sqrt{\gamma^2 - 4\alpha\beta})/(2\alpha)$.

Thus, any equilibrium point of the Rössler system where $\alpha \neq 0$ must be $\Big((\gamma \pm \sqrt{\gamma^2 - 4\alpha\beta})/2, (-\gamma \mp \sqrt{\gamma^2 - 4\alpha\beta})/(2\alpha), (\gamma \pm \sqrt{\gamma^2 - 4\alpha\beta})/(2\alpha)\Big)$. Of course, the equilibrium points are only real if $\gamma^2 - 4\alpha\beta \geq 0$.

If $\alpha = 0$, then any equilibrium point of the Rössler system where $\gamma \neq 0$ must be $(0, -\beta/\gamma, \beta/\gamma)$.

If $\alpha = \gamma = 0$, then any equilibrium point of the Rössler system must be $(0, -z_e, z_e)$ where $z_e \in \mathbb{R}$. However, this is only possible if $\beta = 0$

□

Rössler first used the parameters $\alpha = 0.2$, $\beta = 0.2$, and $\gamma = 5.7$ in order to generate his attractor. With these parameters, the Rössler system has the approximate equilibrium points (5.693, -28.465, 28.465) and (0.007,-0.035, 0.035). It is interesting to note that the Rössler Attractor only circles around the latter of these equilibrium points, not both like in previous examples. In this case, the attractor is shaped like a mobius strip around this single equilibrium point, connecting the outer-most edge of the upward-rising "flair" with the inner-most edge of the horizontal spiral. This is exemplified in Figure 4.

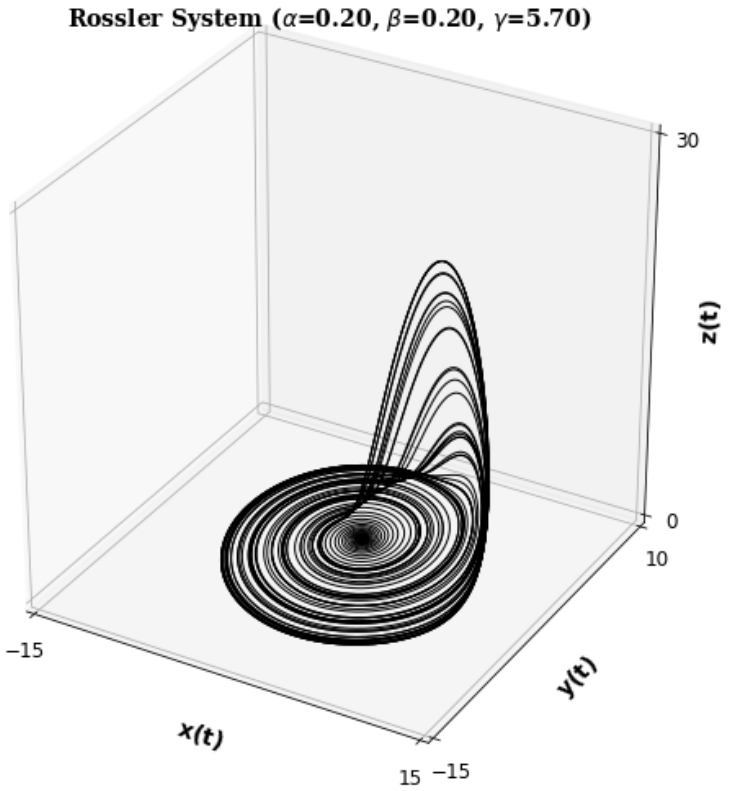

Figure 4: *The Rössler Attractor, developed from the unstable manifolds of the equilibrium points* $(0.007, -0.035, 0.035)$*, where* $\alpha = 0.2$*,* $\beta = 0.2$*, and* $\gamma = 5.7$ *[16].*

ii. Chaos Theory and Strange Attractors

All the strange attractors featured in the previous subsection have been chosen specifically, as they also exhibit a very interesting phenomenon: chaos. In order to define chaos, we must first understand a concept central to chaotic dynamical systems.

Chaos in essence has to do with how microscopic differences in initial conditions can lead to macroscopic differences in the resulting trajectories given enough time. Let us say we have the system of differential equations $\dot{\mathbf{x}} = \mathbf{F}(\mathbf{x}, t)$ with corresponding dynamical system $\mathbf{x}(t) = \delta(\mathbf{x}(0), t)$. Say we have a reference trajectory $\mathbf{x}_1(t)$ and a perturbed trajectory $\mathbf{x}_2(t)$, where $\varepsilon(t) = |\mathbf{x}_1(t) - \mathbf{x}_2(t)|$. We assume that $\varepsilon(0) \ll 1$. We then define the maximum Lyapunov exponent as the eventual exponential rate of expansion [2].

$$\lambda(\mathbf{x}_1(0)) = \lim_{t\to\infty} \lim_{\varepsilon(0)\to 0} \frac{1}{t} \ln\left(\frac{\varepsilon(t)}{\varepsilon(0)}\right) \tag{8}$$

With this equation in mind, we can easily define chaos.

Definition II.8 (**Chaos**). *Chaos is the phenomenon where a dynamical system is extremely sensitive to initial conditions in some set* $C \subseteq \mathbb{R}^n$. *Mathematically,* C *exhibits chaos if for all* $\mathbf{x} \in C$, *the maximal Lyapunov exponent* $\lambda(\mathbf{x})$ *is positive [2].*[1]

Simply put, let's say we have two trajectories in a dynamical system with extremely similar (yet distinct) initial conditions. If these trajectories are found in a chaotic subspace of the phase plane, then chaos dictates that the microscopic difference in initial conditions will eventually result in macroscopic differences between the trajectories [2][23].

As an example of the Lorenz Attractor's chaotic nature, we present a simple but effective situation. Suppose we take the Lorenz system defined in Equation (4) with the same parameters declared in Figure 2. We then plot two trajectories $\mathbf{x}_1(t)$ and $\mathbf{x}_2(t)$ with initial conditions that are $\varepsilon(0) = |\mathbf{x}_1(0) - \mathbf{x}_2(0)| = 10^{-5}$ apart. Figure 5 then shows the component-wise progression of $\mathbf{x}_1(t)$ and $\mathbf{x}_2(t)$.

[1]The authors are aware of the existence of a dynamical system's Lyapunov spectrum. However, we do not see the need of characterizing systems as hyperchaotic or not, and thus find it sufficient to just define the maximal Lyapunov exponent for the purposes of this document. For more information, see [2][21]

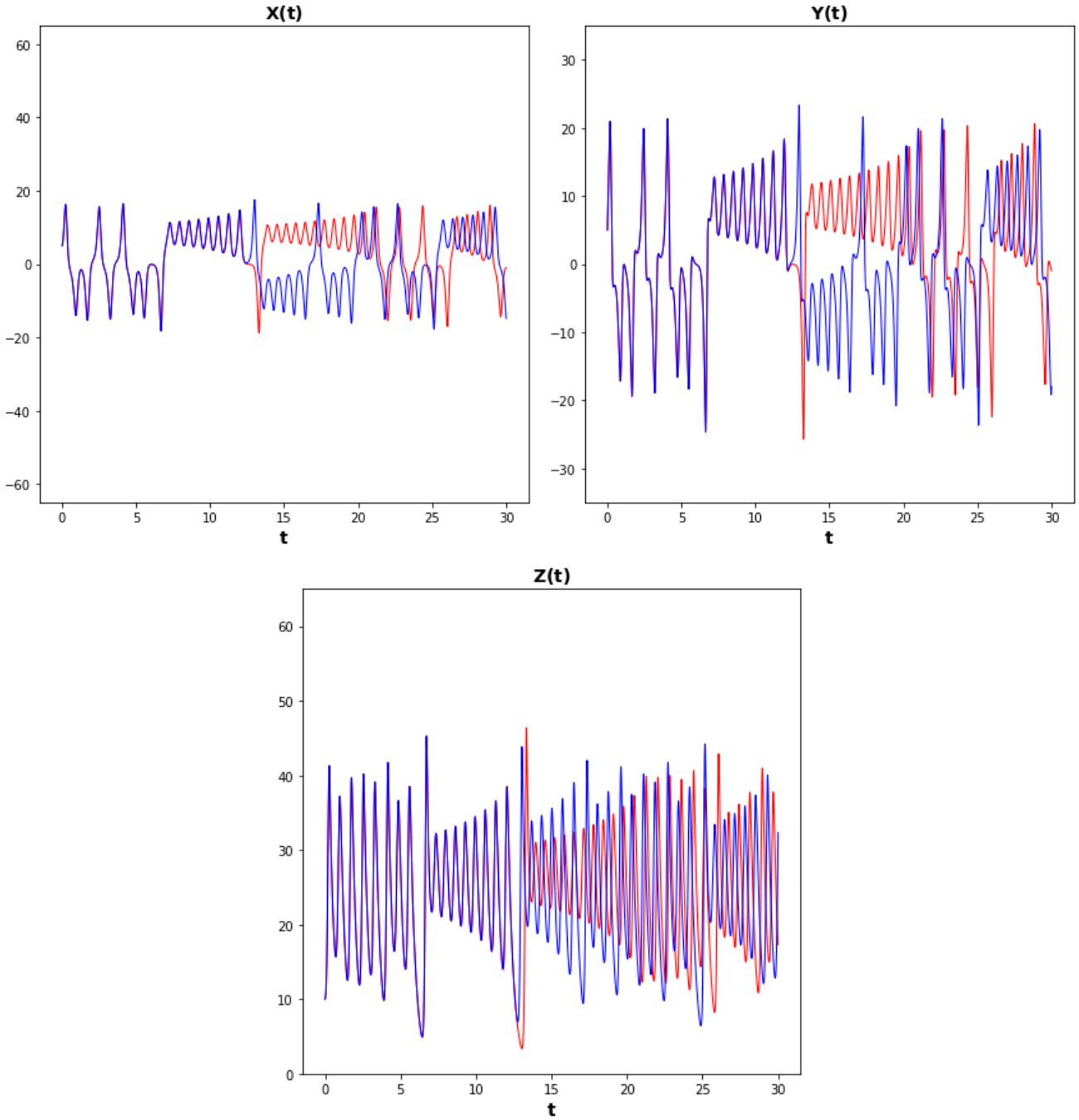

Figure 5: *The component-wise progression of* $\mathbf{x}_1(t)$ *(in red) and* $\mathbf{x}_2(t)$ *(in blue) in the Lorenz system when* $\sigma = 10$*,* $\rho = 28$*, and* $\beta = 8/3$*. These plots were generated with and RK14(10) method using a timestep of* 0.001 *[8][9].*

One can easily notice the difference between $\mathbf{x}_1(t)$ and $\mathbf{x}_2(t)$ after a certain amount of time has passed. Because of the extraordinarily accurate numerical integration

method used in developing these figures, the difference between the trajectories can only be a result of the chaotic nature of the Lorenz Attractor.

As a point of interest, one could assume that all strange attractors are chaotic, but this is not the case. We can prove this by simply giving an example of the contrary. The discrete Feigenbaum Attractor is an example of a strange attractor that is in fact not chaotic [2]. Thus, we can see that chaos is present in many strange attractors, but it can not be used to truly define a strange attractor.

Chaotic attractors in particular, because of their intriguing behavior and occurrence in many areas of science, are phenomena that are on the foreground of modern mathematical research. One of the current topics in this field of research is the localization of these attractors: determining which sets of the phase space could contain an attractor and which sets cannot. In the next section, we will be exploring some current localization techniques currently in use. Then we will explore a new localization technique that has surfaced in recently years, showing potential in easily localizing chaotic attractors in a great many systems.

III. Current Methods of Localization

Localization can be seen as narrowing down the location of a strange attractor, should it exist [4][17]. The usefulness of localization can be explained with a thought experiment. Say we have a dynamical system and we wish to investigate whether this system under a certain set of parameters contains a strange chaotic attractor. Instead of searching the entire n-dimension phase space, we apply a localization analysis over our dynamical system. In this way, we only need to investigate the regions permitted by the localization analysis to potentially contain a strange attractor, and ignore the rest. This would speedup the search for a strange attractor significantly.

Here we present an overview of a number of localization techniques.

i. Localization through Plotting of Trajectories

The easiest method of localizing a strange attractor is by simply plotting a trajectory with an initial condition in the basin of attraction of the attractor itself. Chaos may force the trajectory to lose accuracy to the true solution, but for localization this hardly posses a problem; the trajectory will still give a clear picture of the structure and location of the attractor.

The issue is then determining the basins of attraction for each attractor. In general, this is not an easy task. Basins of attraction can be frustratingly small and difficult to find. One could brute-force the issue by plotting a large number of trajectories scattered throughout the phase space, but this is extremely costly; the number of trajectories needed for this approach would be too enormous for this method to be considered viable.

In light of this, we divide attractors into two different categories: self-excited and hidden, the definitions of which are given in Definition II.7 Localizing a self-excited attractor only requires plotting the unstable manifolds of an equilibrium point in its basin of attraction; at least one of the manifolds will enter the attractor after a finite period of time, thus showing the location and structure of the attractor. Figures 2, 3, and 4 from Section II are perfect examples of this technique.

Hidden attractors, on the other hand, are much more complicated to localize, as they can in theory be located anywhere in the phase space without an equilibrium point to "anchor" them down. One way of localizing a hidden attractor is by simplifying the system of differential equations substantially and analytically computing a rough approximation. Using this rough approximate, we iteratively refine it, leading to

a much more accurate approximation of our hidden attractor. We highlight this method below.

i.1 Localization of Hidden Attractors

This method is described entirely in [10] and [12], where the authors of the article apply their technique to differential systems of the form

$$\dot{\mathbf{x}} = P\mathbf{x} + \phi(\mathbf{x}) \tag{9}$$

Here, $\mathbf{x}(t) \in \mathbb{R}^n$, $P \in \mathbb{R}^{n\times n}$ is a constant matrix, and $\phi : \mathbb{R}^{n\times n} \to \mathbb{R}^{n\times n}$ is a continuous vector function with $\phi(\mathbf{0}) = \mathbf{0}$ [10][12].

Now, say there exists some matrix $K \in \mathbb{R}^{n\times n}$ so that $P_0 = P + K$ has two purely imaginary eigenvalues called $\pm i\omega_0$ with $\omega_0 \in \mathbb{R}$. We also require that the rest of the eigenvalues of P_0 all have negative real parts. We can then rewrite Equation (9) into the following form. For purposes that we shall explain later, we also introduce a new variable ε that ranges from 0 to 1.

$$\begin{aligned} &\dot{\mathbf{x}} = P_0\mathbf{x} + \varepsilon\varphi(\mathbf{x}) \\ &\text{where } \varphi(\mathbf{x}) = \phi(\mathbf{x}) - K\mathbf{x} \end{aligned} \tag{10}$$

Notice that if $\varepsilon = 1$, the Equation (9) and Equation (10) are equivalent.

Lets say for $\varepsilon = 0$ that our system contains a periodic attractor, one that we can analytically compute. We can then increase ε by a sufficiently small increment, resulting in a dynamical system that has been slightly augmented. We assume, since this augmentation was small, that the periodic attractor has been slightly augmented as well, resulting in a new (pseudo-)periodic attractor. If the increase to ε was sufficiently small, then it stands to reason that any point $\mathbf{x}_0$ on our original periodic attractor will be in the basin of attraction of this new (pseudo-)periodic attractor. Thus, we can plot a trajectory from $\mathbf{x}_0$ and with it approximate our new attractor after a transient amount of time [10][12].

Please note that it is very possible that increasing ε beyond a certain value may result in a bifurcation in our dynamical system that destroys our attractor. We have no guarantees that our attractor will stay intact.

We then increase our ε over and over, using a point in the attractor that was just found (assuming it exists) as an initial condition for a trajectory under Equation (10). This trajectory will then wander into the new attractor for the system (assuming it

exists) since the increase of ε was chosen small enough to where our initial condition of the trajectory can be found in this new attractor's basin of attraction. We can continue to do this until either any increase in ε augments the system of equations enough to where the attractor disintegrates entirely, or to where $\varepsilon = 1$. If the latter happens, then we have found an attractor for Equation (9). If this attractor does not contain any equilibrium points in its basin of attraction, then it must be a hidden attractor [10][12].

We show this process in more detail with an example taken from [10] and [12]. Suppose we have the following system

$$\begin{cases} \dot{x} = \alpha(y - x - f(x)) \\ \dot{y} = x - y + z \\ \dot{z} = -\beta y - \gamma z \end{cases} \tag{11}$$

where $\alpha = 8.4562$, $\beta = 12.0732$, $\gamma = 0.0052$, and $f(x)$ is defined as in Equation (6) with $m_0 = -0.1768$ and $m_1 = -1.1468$. Notice that this system is very similar to that defined in Equation (5) when $\gamma = 0$. Therefore, we shall refer to this system as a form of a Chua system [10][12].

Following the form presented in Equation (9), we can rewrite our Chua system into the following form [10][12].

$$\begin{aligned} &\dot{\mathbf{x}} = P\mathbf{x} + \mathbf{q}\phi(\mathbf{r}^T\mathbf{x}) \\ &\text{where } \phi(\mathbf{r}^T\mathbf{x}) = (m_0 - m_1)\left(|\mathbf{r}^T\mathbf{x} + 1| - |\mathbf{r}^T\mathbf{x} - 1|\right)/2 \\ &\text{and} \\ &P = \begin{bmatrix} -\alpha(m_1+1) & \alpha & 0 \\ 1 & -1 & 1 \\ 0 & -\beta & -\gamma \end{bmatrix}, q = \begin{bmatrix} -\alpha \\ 0 \\ 0 \end{bmatrix}, r = \begin{bmatrix} 1 \\ 0 \\ 0 \end{bmatrix} \end{aligned} \tag{12}$$

Now, let us define matrix P_0 and function φ for this system while introducing a new variable $\varepsilon \in [0, 1]$. For $k \in \mathbb{R}$

$$\begin{aligned} &\dot{\mathbf{x}} = P_0\mathbf{x} + \varepsilon\mathbf{q}\varphi(\mathbf{r}^T\mathbf{x}) \text{ where} \\ &P_0 = P + k\mathbf{q}\mathbf{r}^T = \begin{bmatrix} -\alpha(m_1 + 1 + k) & \alpha & 0 \\ 1 & -1 & 1 \\ 0 & -\beta & -\gamma \end{bmatrix}, \\ &\varphi(\mathbf{r}^T\mathbf{x}) = \phi(\mathbf{r}^T\mathbf{x}) - k\mathbf{r}^T\mathbf{x} \end{aligned} \tag{13}$$

where k is chosen so that the eigenvalues of P_0 are equal to $i\omega_0$, $-i\omega_0$, and $-d$, where $\omega_0 \in \mathbf{R}_{\geq 0}$ and $Re(d) \in \mathbf{R}_{>0}$ [10][12]. Notice that Equation (12) and Equation (13)

are equivalent when $\varepsilon = 1$.

In order to compute the variables ω_0, k, and d, we introduce a concept from system and control theory: the transfer function[2]. In this case, the transfer function can be defined as

$$W_P(p) = \mathbf{r}^T(P - pI)^{-1}\mathbf{q} \text{ with } p \in \mathbb{C} \tag{14}$$

Then [10] and [12] state that $Im(W_P(\pm i\omega_0)) = 0$ and $k = -Re(W_P(\pm i\omega_0))^{-1}$, giving a method of at least approximating the values of ω_0 and the corresponding values of k. Then, using a result from linear algebra, we can see that

$$d = \frac{det(P_0)}{-\omega_0^2} = \frac{\alpha(m_1 + k + 1)(\beta + \gamma) - \alpha\gamma}{\omega_0^2}$$

The system defined in Equation (13) may contain a hidden attractor, but finding it in its current form can be difficult. Therefore, we apply the invertible linear transformation $\mathbf{x} = S\mathbf{y}$, with $S \in \mathbb{R}^{n\times n}$ and $\mathbf{y} \in \mathbb{R}^n$.

$$\begin{aligned}
\dot{\mathbf{x}} &= P_0\mathbf{x} + \varepsilon\mathbf{q}\varphi(\mathbf{r}^T\mathbf{x}) \\
&\Leftrightarrow \\
S^{-1}\dot{\mathbf{x}} &= \left(S^{-1}P_0S\right)S^{-1}\mathbf{x} + \varepsilon(S^{-1}\mathbf{q})\varphi\left((\mathbf{r}^TS)S^{-1}\mathbf{x}\right) \\
&\Leftrightarrow \\
\dot{\mathbf{y}} &= A\mathbf{y} + \varepsilon\mathbf{b}\varphi(\mathbf{c}^T\mathbf{y})
\end{aligned}$$

Here, $A = S^{-1}P_0S$, $b = S^{-1}q$, and $c^T = r^TS$. In order to fully determine what S should be, we must first concretely define A, $\mathbf{b}$, and $\mathbf{c}$. We do so as follows [10][12].

$$\begin{aligned}
&\dot{\mathbf{y}} = A\mathbf{y} + \varepsilon\mathbf{b}\varphi(\mathbf{c}^T\mathbf{y}) \\
&\text{where } \varphi(\mathbf{c}^T\mathbf{y}) = (m_0 - m_1)\left(|\mathbf{c}^T\mathbf{y} + 1| - |\mathbf{c}^T\mathbf{y} - 1|\right)/2 - k\mathbf{c}^T\mathbf{y} \\
&\text{and} \\
&A = \begin{bmatrix} 0 & -\omega_0 & 0 \\ \omega_0 & 0 & 0 \\ 0 & 0 & -d \end{bmatrix},\ b = \begin{bmatrix} b_1 \\ b_2 \\ 1 \end{bmatrix},\ c = \begin{bmatrix} 1 \\ 0 \\ h \end{bmatrix},\ \text{where } b_1, b_2, h \in \mathbb{R}
\end{aligned} \tag{15}$$

The reason for this definition comes in the form of a theorem.

Theorem III.1. *Say we have the system defined in Equation* (13) *with* $\varepsilon = 0$*, and where* ω_0 *and* k *are concretely defined. If there exists an* $a_0 \in \mathbb{R}$ *so that*

$$\Phi(a_0) = \int_0^{2\pi/\omega_0} \varphi(a_0\cos(\omega_0 t))\left(b_1\cos(\omega_0 t) + b_2\sin(\omega_0 t)\right)dt = 0$$

[2]The physical interpretation of this function is not important for this document and therefore is omitted here. For an introduction into transfer functions, see [1]

and that $\Phi'(a_0) < 0$*, then there exists a periodic solution in Equation* (13) *(with* $\varepsilon = 0$*) with initial condition* $[x(0), y(0), z(0)]^T = S[a_0, 0, 0]^T$ *[12].*

We will use this periodic solution to hopefully construct a hidden attractor in Equation (12), if one exists.

Of course, S must first be defined before any further progress can be made. Therefore, after numerous calculations, we can conclude from [10] that

$$S = \begin{bmatrix} 1 & 0 & -h \\ m_1 + k + 1 & \frac{-\omega_0}{\alpha} & \frac{h}{\alpha}(d - \alpha(k + m_1 + 1)) \\ m1 + k - \frac{\omega_0^2}{\alpha} & -\omega_0(m_1 + k + 1 + 1/\alpha) & \frac{h}{\alpha}(\alpha + (d - \alpha(m_1 + k + 1))(1 - d)) \end{bmatrix}$$

With this, we can define the the variables b_1, b_2, and h.

$$\begin{aligned} h &= \frac{\alpha\,(\alpha^2(m_1 + k + 1)^2 + \alpha + \omega_0^2)}{\omega_0^2 + d^2} \\ b1 &= h - \alpha \\ b2 &= \frac{dh - \alpha^2(m_1 + k + 1)}{\omega_0} \end{aligned}$$

Having completely defined every variable in Equation (15), we can finally numerically localize the hidden attractor in Equation (11). The most pivotal step is defining ω_0 and the corresponding value for k using the transfer function given in Equation (14), and then approximate the corresponding value for a_0 from Theorem III.1, if it exists. Numerically, we find not one, but two sets of appropriate parameters, given below.

$$\begin{aligned} (\omega_0^{(1)},\ k^{(1)},\ a_0^{(1)}) &= (2.0392, 0.2099, 5.8499) \\ (\omega_0^{(2)},\ k^{(2)},\ a_0^{(2)}) &= (3.2454, 0.9598, 1.0422) \end{aligned}$$

Therefore, since we have two sets of parameters, we can find at most two hidden attractors in Equation 11 using this method. We first focus on the first set of parameters $\omega_0^{(1)}$, $k^{(1)}$, and $a_0^{(1)}$).

From Theorem III.1, we see that the system defined in Equation (13) with $\varepsilon = 0$ has a periodic solution with the initial condition $\mathbf{x}(0) = (5.8499, 0.3690, -8.3577)$. This periodic solution is given in Figure 6.

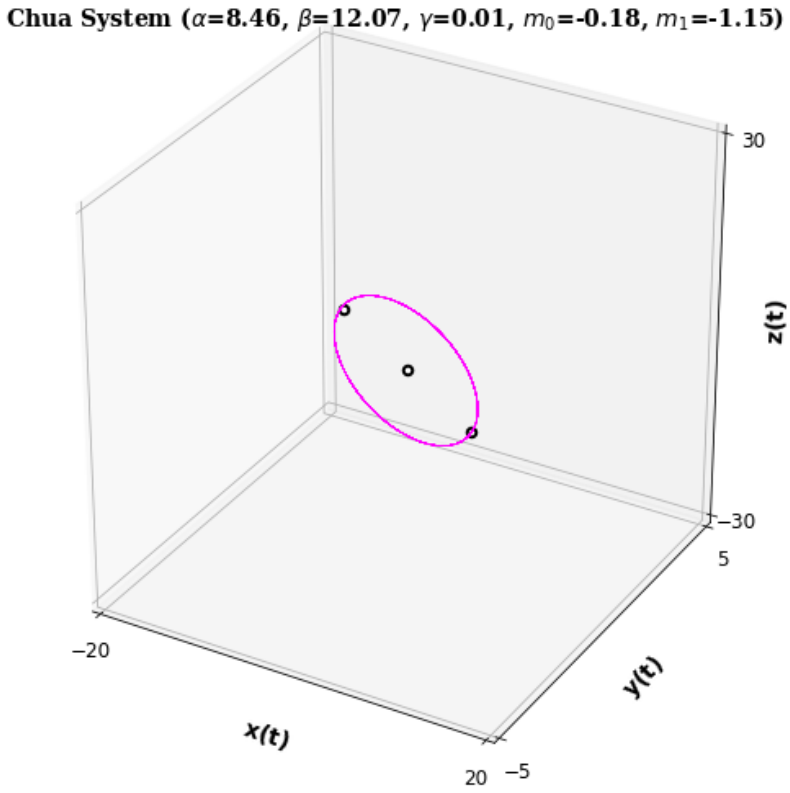

Figure 6: *A periodic solution of the system described in Equation* (13) *using* $\omega_0^{(1)}$, $k^{(1)}$, $a_0^{(1)}$, *and* $\varepsilon = 0$, *starting at initial condition* $\mathbf{x}(0) = (5.8499, 0.3690, -8.3577)$.

We can take any point along the periodic orbit shown in Figure 6 and use it as the initial condition of a trajectory in Equation (13), increasing ε incrementally. If ε is increased by a sufficiently small amount, this new trajectory should start somewhere in the basin of attraction of the new (pseudo-)periodic attractor, should it exist. We chose to increase ε from 0 to 0.2. Figure 7 then shows the progress of this new trajectory and the (pseudo-)periodic attractor it falls into.

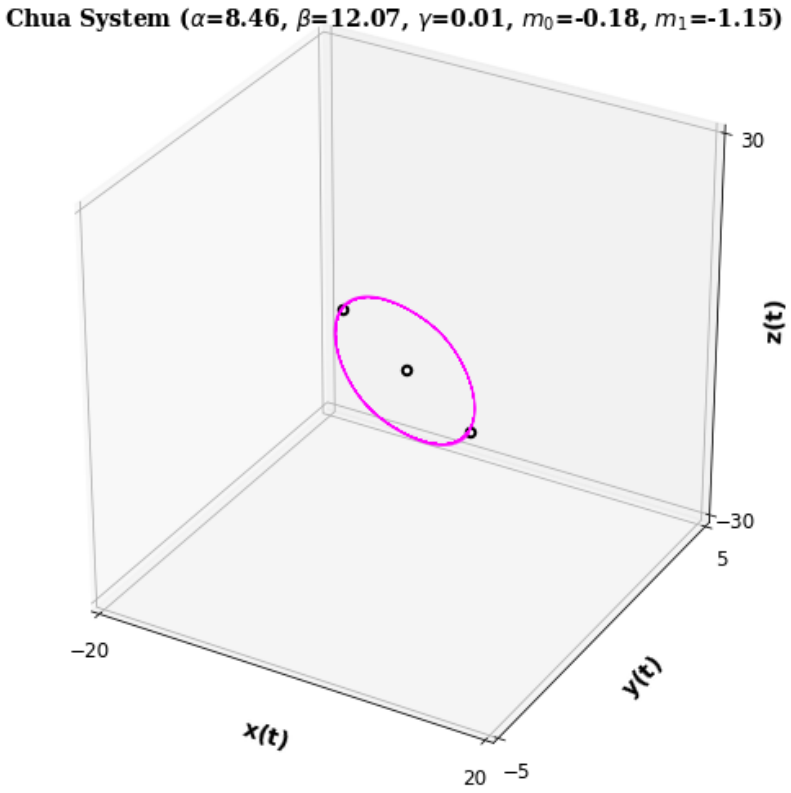

Figure 7: *The (pseudo-)periodic solution of the system described in Equation* (13) *using* $\omega_0^{(1)}$, $k^{(1)}$, $a_0^{(1)}$, *and* $\varepsilon = 0.2$.

We can again take any point along the (pseudo-)periodic attractor shown in Figure 7 and use it as the initial condition of a trajectory in Equation (13), increasing ε from 0.2 to 0.4. Figure 8 shows the progress of this new trajectory and the (pseudo-)periodic attractor it falls into.

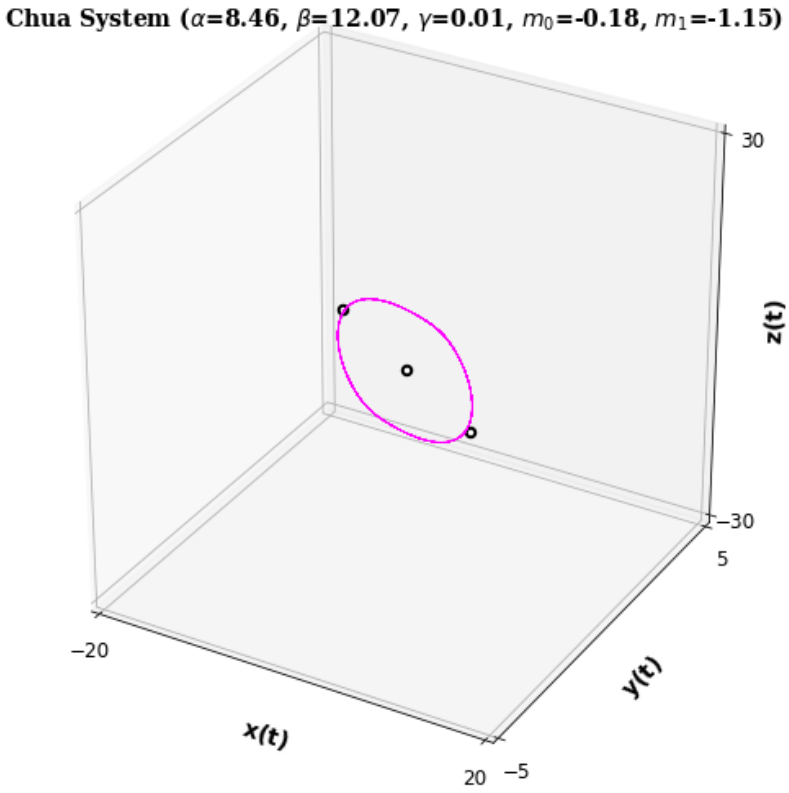

Figure 8: *The (pseudo-)periodic solution of the system described in Equation* (13) *using* $\omega_0^{(1)}$, $k^{(1)}$, $a_0^{(1)}$, *and* $\varepsilon = 0.4$.

We can yet again take any point along the (pseudo-)periodic attractor shown in Figure 8 and use it as the initial condition of a trajectory in Equation (13), increasing ε from 0.4 to 0.6. Figure 9 shows the progress of this new trajectory and the (pseudo-) periodic attractor it falls into.

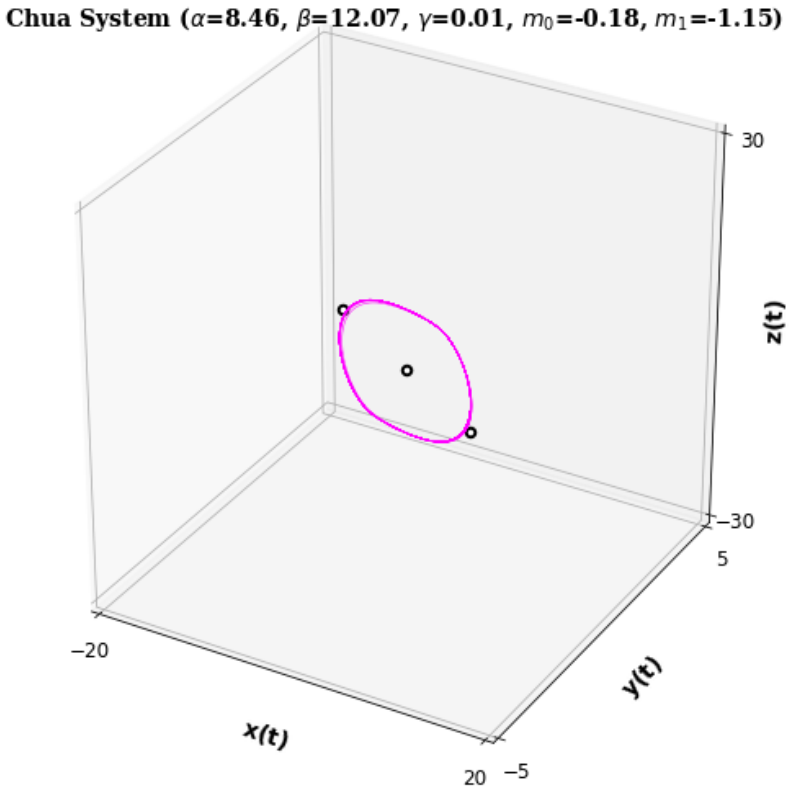

Figure 9: *The (pseudo-)periodic solution of the system described in Equation* (13) *using* $\omega_0^{(1)}$, $k^{(1)}$, $a_0^{(1)}$, *and* $\varepsilon = 0.6$.

We can again take any point along the (pseudo-)periodic attractor shown in Figure 9 and use it as the initial condition of a trajectory in Equation (13), increasing ε from 0.6 to 0.8. Figure 10 shows the progress of this new trajectory and the (pseudo-)periodic attractor it falls into. Notice that the structure of this (pseudo-)periodic attractor is starting to resemble something less like a limit cycle and more like a strange attractor.

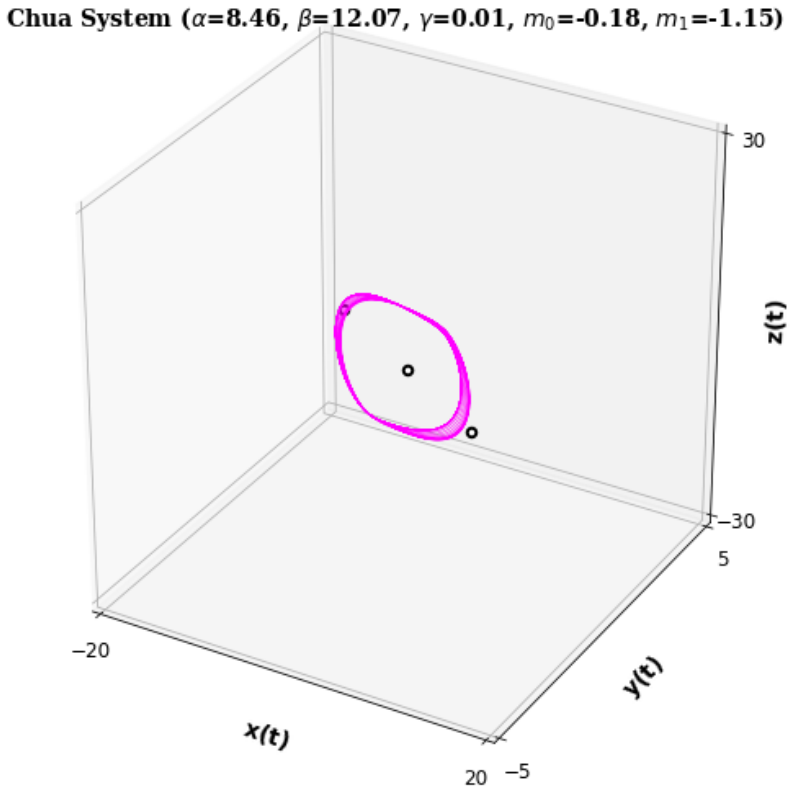

Figure 10: *The (pseudo-)periodic solution of the system described in Equation* (13) *using* $\omega_0^{(1)}$, $k^{(1)}$, $a_0^{(1)}$, *and* $\varepsilon = 0.8$.

Finally, we can again take any point along the attractor shown in Figure 10 and use it as the initial condition of a trajectory in Equation (13), increasing ε from 0.8 to 1. Notice that when $\varepsilon = 1$, Equation (13) is equivalent to Equation (12). Figure 11 shows the progress of this new trajectory and the strange attractor it falls into.

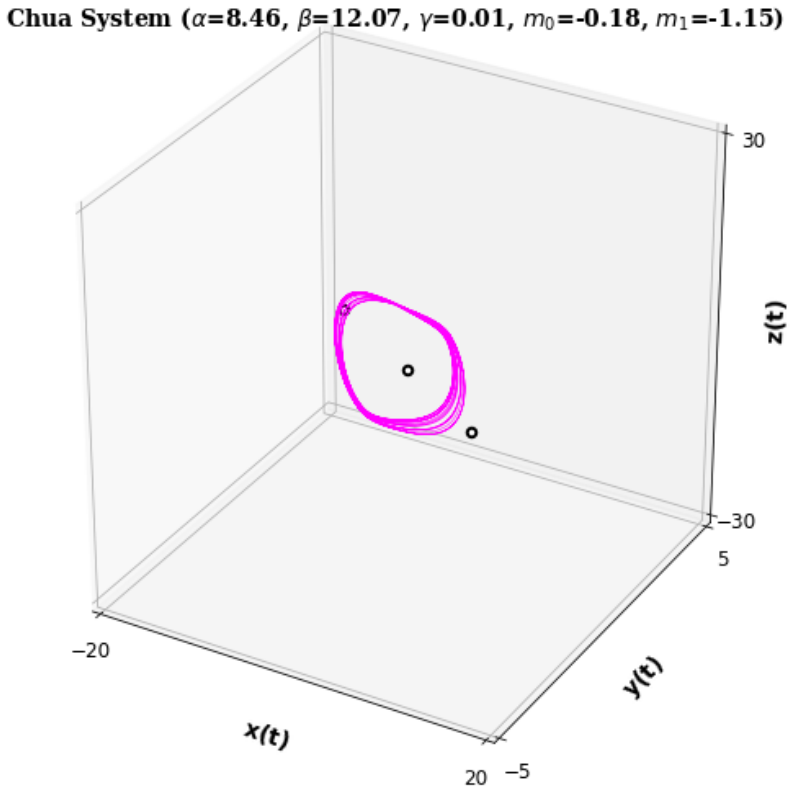

Figure 11: *An attractor of the Chua system described in Equation* (11)*. Since the maximal Lyapunov Exponents of this attractors is larger than 0.0 (calculations not shown), we can conclude that this is a chaotic attractors of our Chua system.*

We can also use the same technique for the second set of parameters ($\omega_0^{(2)}$, $k^{(2)}$, $a_0^{(2)}$). Through careful manipulation of ε, we can approximate a second attractor of our Chua system, which we show in Figure 12.

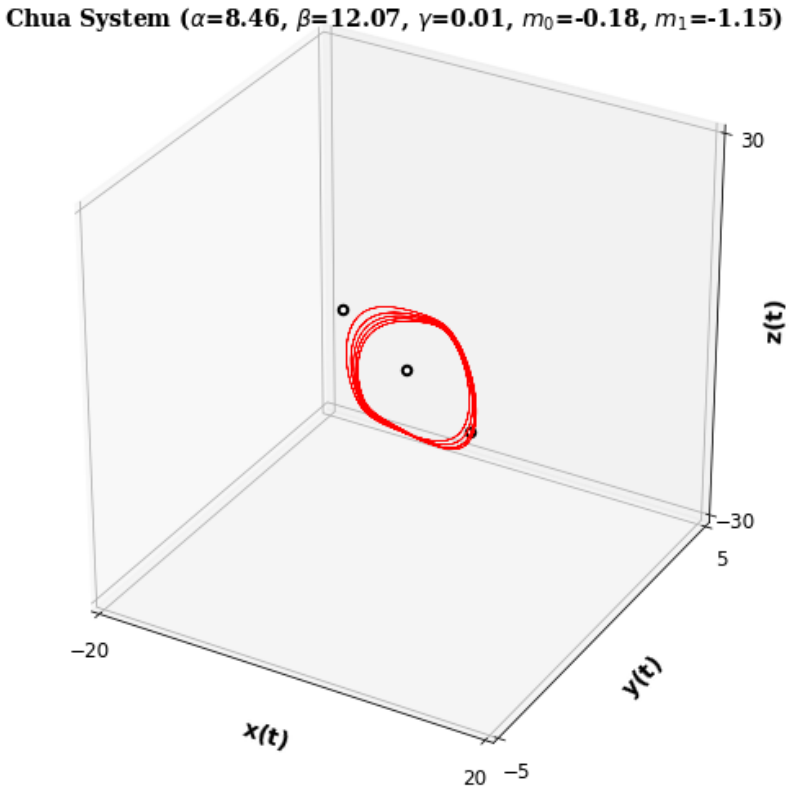

Figure 12: *Another attractor of the Chua system described in Equation* (11)*. Since the maximal Lyapunov Exponents of this attractors is larger than 0.0 (calculations not shown), we can conclude that this is a chaotic attractors of our Chua system.*

Together, along with plotting the manifolds of the three equilibrium points of the system, we can show how our Chua system behaves in Figure 13 [10][12].

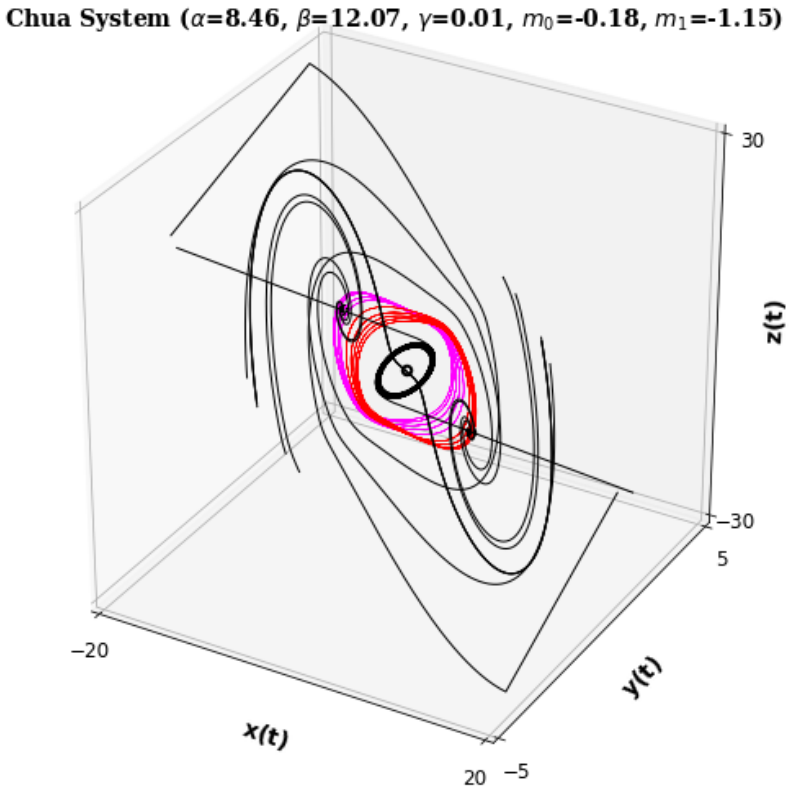

Figure 13: *The Chua system described in Equation* (11)*, showing the attractors (in red and magenta) as well as the manifolds of the three equilibrium points (in black). Since none of the manifolds of the equilibria fall into our two attractors, we can conclude that these attractors must be hidden chaotic attractors.*

Notice that this method is generally applicable to all systems that can be described by Equation (9), making this method very generally applicable. However, this method gives no guarantees that a hidden attractor will exist in a particular system, only that if it exists there is the potential of approximating it incrementally. These increments are dependent on ε, and thus great care must be taken in increasing ε during every step of the algorithm.

On a different note, we saw that each step in this method required a considerable amount of analytic prowess. Our differential system of equations needed to be transformed multiple times, each transformation having its advantages and disadvantages. Perhaps it would be better to use a different method that is not as academically taxing.

In conclusion, using trajectories to map out the structure of a strange attractor can be very effective. For self-excited attractors, can be very simple: plot out all unstable manifolds of all equilibria of the dynamical system and see if any of the manifolds fall into an attractor of the system. For hidden attractors, this process is much more complicated and requires more sophisticated methods.

ii. Nambu Hamiltonians

This method involves the use of Nambu mechanics, a generalization of Hamiltonian mechanics, which are commonplace in mechanical physics. We first give the definition for a Hamiltonian system. Then we expand upon it using the Nambu formalism, but only focusing on the 3-dimensional case for simplicity's sake; for a more complete definition, see [20].

Definition III.1. ***Hamiltonian System***
Suppose $\mathbf{x}(t) \in A$ *and* $\mathbf{y}(t) \in B$ *for* $t \in \mathbb{R}$*, with* $A \subseteq \mathbb{R}^n$ *and* $B \subseteq \mathbb{R}^n$*. Suppose there exists a function* $H : A \times B \to \mathbb{R}$ *with* $H \in \mathcal{C}^1(A, B)$ *so that we can define the* $2n$*-dimensional system of equations*

$$\begin{cases} \dot{\mathbf{x}} = \dfrac{\partial H}{\partial \mathbf{y}} = \left(\dfrac{\partial H}{\partial y_1}, \cdots, \dfrac{\partial H}{\partial y_n} \right)^T \\ \dot{\mathbf{y}} = -\dfrac{\partial H}{\partial \mathbf{x}} = -\left(\dfrac{\partial H}{\partial x_1}, \cdots, \dfrac{\partial H}{\partial x_n} \right)^T \end{cases}$$

This is known as a Hamiltonian system with n*-degrees of freedom, where* H *is the Hamiltonian of the system [15].*

Notice that in a Hamiltonian System,

$$\dot{H} = \frac{\partial H}{\partial \mathbf{x}}\dot{\mathbf{x}} + \frac{\partial H}{\partial \mathbf{y}}\dot{\mathbf{y}} = -\dot{\mathbf{y}}\dot{\mathbf{x}} + \dot{\mathbf{x}}\dot{\mathbf{y}} = 0$$

We can conclude that $H(\mathbf{x}(t), \mathbf{y}(t)) = H(\mathbf{x}(0), \mathbf{y}(0))$ for all $t \in \mathbf{R}$. This means that for any trajectory in our system, the value of H remains constant.

We can also see it a different way. The equation $H(\mathbf{x}(t), \mathbf{y}(t)) = H(\mathbf{x}(0), \mathbf{y}(0))$ defines a surface in the phase plane. If a trajectory of our system were to have the initial condition $(\mathbf{x}(0), \mathbf{y}(0))$, then the trajectory would have to remain on this surface for all $t \in \mathbf{R}$.

As one can see, using the Hamiltonian is an incredibly efficient way to localize the trajectories of a system. However, it is not always possible to find a Hamiltonian

function. Even when it is possible, calculating a suitable Hamiltonian is usually a very difficult task.

We now expand on the concept of a Hamiltonian system by introducing what we call Nambu systems. For simplicity, we only focus on 3-dimensional Nambu systems; for a more complete definition, see [20].

Definition III.2. ***Nambu System for 3 Dimensions***
Suppose $\mathbf{x}(t) = (x(t), y(t), z(t)) \in A$ *for* $t \in \mathbb{R}$, *with* $A \subseteq \mathbb{R}^3$. *Suppose there exist functions* $H_1, H_2 : A \to \mathbb{R}$ *with* $H_1, H_2 \in \mathcal{C}^1(A)$ *so that we can define the 3-dimensional system of equations*

$$\begin{cases} \dot{x} = \dfrac{\partial H_1}{\partial y}\dfrac{\partial H_2}{\partial z} - \dfrac{\partial H_1}{\partial z}\dfrac{\partial H_2}{\partial y} \\ \dot{y} = \dfrac{\partial H_1}{\partial z}\dfrac{\partial H_2}{\partial x} - \dfrac{\partial H_1}{\partial x}\dfrac{\partial H_2}{\partial z} \\ \dot{z} = \dfrac{\partial H_1}{\partial x}\dfrac{\partial H_2}{\partial y} - \dfrac{\partial H_1}{\partial y}\dfrac{\partial H_2}{\partial x} \end{cases}$$

We call this a 3-dimensional Nambu system, where H_1 *and* H_2 *are the "Nambunians" of the system (this naming is a personal choice by the authors and is not reflected in other literature). Notice that we can reduce this definition significantly into the equation* $\dot{\mathbf{x}} = \nabla H_1 \times \nabla H_2$, *where "*$\times$*" signifies the cross-product [17][20].*

We now introduce and prove a few lemmas for 3-dimensional Nambu Systems.

Lemma III.2. *Suppose we have a Nambu system as described in definition III.2. Then* $\dot{H}_1 = \dot{H}_2 = 0$

Proof. We prove this for H_1 only. The proof for H_2 is extremely similar.

$$\begin{aligned}
\dot{H}_1 &= \frac{\partial H_1}{\partial x}\dot{x} + \frac{\partial H_1}{\partial y}\dot{y} + \frac{\partial H_1}{\partial z}\dot{z} \\
&= \frac{\partial H_1}{\partial x}\left(\frac{\partial H_1}{\partial y}\frac{\partial H_2}{\partial z} - \frac{\partial H_1}{\partial z}\frac{\partial H_2}{\partial y}\right) \\
&\quad + \frac{\partial H_1}{\partial y}\left(\frac{\partial H_1}{\partial z}\frac{\partial H_2}{\partial x} - \frac{\partial H_1}{\partial x}\frac{\partial H_2}{\partial z}\right) \\
&\quad + \frac{\partial H_1}{\partial z}\left(\frac{\partial H_1}{\partial x}\frac{\partial H_2}{\partial y} - \frac{\partial H_1}{\partial y}\frac{\partial H_2}{\partial x}\right) \\
&= \frac{\partial H_1}{\partial x}\frac{\partial H_1}{\partial y}\frac{\partial H_2}{\partial z} - \frac{\partial H_1}{\partial x}\frac{\partial H_1}{\partial z}\frac{\partial H_2}{\partial y} \\
&\quad + \frac{\partial H_1}{\partial y}\frac{\partial H_1}{\partial z}\frac{\partial H_2}{\partial x} - \frac{\partial H_1}{\partial x}\frac{\partial H_1}{\partial y}\frac{\partial H_2}{\partial z} \\
&\quad + \frac{\partial H_1}{\partial x}\frac{\partial H_1}{\partial z}\frac{\partial H_2}{\partial y} - \frac{\partial H_1}{\partial y}\frac{\partial H_1}{\partial z}\frac{\partial H_2}{\partial x} \\
&= 0
\end{aligned}$$

□

Just as before with Hamiltonian systems, we can use Lemma III.2 to conclude that $H_1(x(t), y(t), z(t)) = H_1(x(0), y(0), z(0))$ and $H_2(x(t), y(t), z(t)) = H_2(x(0), y(0), z(0))$, which both describe surfaces in the phase space. As a result, if H_1 and H_2 are distinct, the trajectory with initial condition $(x(0), y(0), z(0))$ must lie in the intersection of these two equations. Therefore, if one knows the Nambunians of a Nambu system, they are able to very accurately predict where any trajectory will be in the phase space [17].

Lemma III.3. *Suppose we have a Nambu system as described in definition III.2. Suppose $\mathcal{H}_1$ and $\mathcal{H}_2$ are continuously differentiable functions of H_1 and H_2, where the corresponding Jacobian has a determinant of 1. Then $\mathcal{H}_1$ and $\mathcal{H}_2$ can be used instead of H_1 and H_2 in Definition III.2.*

Proof. Suppose we have a Nambu system described in Definition III.2, where $\mathbf{x} = \nabla H_1 \times \nabla H_2$. Suppose we have continuously differentiable functions $\mathcal{H}_1(H_1, H_2)$ and $\mathcal{H}_2(H_1, H_2)$ where

$$\left|\frac{\partial(\mathcal{H}_1, \mathcal{H}_2)}{\partial(H_1, H_2)}\right| = \frac{\partial \mathcal{H}_1}{\partial H_1}\frac{\partial \mathcal{H}_2}{\partial H_2} - \frac{\partial \mathcal{H}_1}{\partial H_2}\frac{\partial \mathcal{H}_2}{\partial H_1} = 1$$

We take a look at $\nabla\mathcal{H}_1 \times \nabla\mathcal{H}_2$, which is a 3-dimensional vector. We focus on each of its elements $(\nabla\mathcal{H}_1 \times \nabla\mathcal{H}_2)_1$, $(\nabla\mathcal{H}_1 \times \nabla\mathcal{H}_2)_2$, and $(\nabla\mathcal{H}_1 \times \nabla\mathcal{H}_2)_3$. Let us start with the first element.

$$\begin{aligned}
(\nabla\mathcal{H}_1 \times \nabla\mathcal{H}_2)_1 &= \frac{\partial\mathcal{H}_1}{\partial y}\frac{\partial\mathcal{H}_2}{\partial z} - \frac{\partial\mathcal{H}_1}{\partial z}\frac{\partial\mathcal{H}_2}{\partial y} \\
&= \left(\frac{\partial\mathcal{H}_1}{\partial H_1}\frac{\partial H_1}{\partial y} + \frac{\partial\mathcal{H}_1}{\partial H_2}\frac{\partial H_2}{\partial y}\right)\left(\frac{\partial\mathcal{H}_2}{\partial H_1}\frac{\partial H_1}{\partial z} + \frac{\partial\mathcal{H}_2}{\partial H_2}\frac{\partial H_2}{\partial z}\right) \\
&\quad - \left(\frac{\partial\mathcal{H}_1}{\partial H_1}\frac{\partial H_1}{\partial z} + \frac{\partial\mathcal{H}_1}{\partial H_2}\frac{\partial H_2}{\partial z}\right)\left(\frac{\partial\mathcal{H}_2}{\partial H_1}\frac{\partial H_1}{\partial y} + \frac{\partial\mathcal{H}_2}{\partial H_2}\frac{\partial H_2}{\partial y}\right) \\
&= \frac{\partial\mathcal{H}_1}{\partial H_1}\frac{\partial H_1}{\partial y}\frac{\partial\mathcal{H}_2}{\partial H_2}\frac{\partial H_2}{\partial z} + \frac{\partial\mathcal{H}_1}{\partial H_2}\frac{\partial H_2}{\partial y}\frac{\partial\mathcal{H}_2}{\partial H_1}\frac{\partial H_1}{\partial z} \\
&\quad - \frac{\partial\mathcal{H}_1}{\partial H_1}\frac{\partial H_1}{\partial z}\frac{\partial\mathcal{H}_2}{\partial H_2}\frac{\partial H_2}{\partial y} - \frac{\partial\mathcal{H}_1}{\partial H_2}\frac{\partial H_2}{\partial z}\frac{\partial\mathcal{H}_2}{\partial H_1}\frac{\partial H_1}{\partial y} \\
&= \left(\frac{\partial\mathcal{H}_1}{\partial H_1}\frac{\partial\mathcal{H}_2}{\partial H_2} - \frac{\partial\mathcal{H}_1}{\partial H_2}\frac{\partial\mathcal{H}_2}{\partial H_1}\right)\left(\frac{\partial H_1}{\partial y}\frac{\partial H_2}{\partial z} - \frac{\partial H_1}{\partial z}\frac{\partial H_2}{\partial y}\right) \\
&= (\nabla H_1 \times \nabla H_2)_1
\end{aligned}$$

In a very similar way, $(\nabla\mathcal{H}_1 \times \nabla\mathcal{H}_2)_2 = (\nabla H_1 \times \nabla H_2)_2$ and $(\nabla\mathcal{H}_1 \times \nabla\mathcal{H}_2)_3 = (\nabla H_1 \times \nabla H_2)_3$. In conclusion, $\dot{\mathbf{x}} = \nabla H_1 \times \nabla H_2 = \nabla\mathcal{H}_1 \times \nabla\mathcal{H}_2$. Therefore, we can replace H_1 with $\mathcal{H}_1$ and H_2 with $\mathcal{H}_2$ in Definition III.2 and still have an equivalent Nambu system. □

Because of Lemma III.3, we can construct an infinite number of Nambunians for a Nambu system. This will be important later on.

In order to show the power of Nambu systems and provide a concrete example as to how they can be used to localize strange attractors, we focus yet again on the Lorenz system as described in Equation (4) with $\sigma = 10$, $\rho = 28$, and $\beta = 8/3$. This example is handled in far greater detail in [17]. We simplify the mathematics here, focusing on understandability.

First of all, the Lorenz system cannot be written as a 3-dimensional Nambu system, the reason for which is simple to explain. Only divergence-free systems have the possibility of being a Nambu system [17]. However, the divergence of the Lorenz system is $\nabla \times \dot{\mathbf{x}} = -(\sigma + 1 + \beta) \neq 0$. Therefore, we must split the system into a "dissipative" (meaning "divergence-containing") part $\mathbf{x}_D$ and a "non-dissipative"

(meaning "divergence-free") part $\mathbf{x}_{ND}$ [17].

$$\begin{cases} \dot{x} = \sigma(y - x) \\ \dot{y} = x(\rho - z) - y \\ \dot{z} = xy - \beta z \end{cases} = \begin{cases} \dot{x}_{ND} = \sigma y_{ND} \\ \dot{y}_{ND} = x_{ND}(\rho - z_{ND}) \\ \dot{z}_{ND} = x_{ND} y_{ND} \end{cases} + \begin{cases} \dot{x}_D = -\sigma x_D \\ \dot{y}_D = -y_D \\ \dot{z}_D = \beta z_D \end{cases} \tag{16}$$

We will focus on the non-dissipative part for now, later reconnecting it with the dissipative part and drawing conclusions from that.

For the non-dissipative part of the Lorenz system, we are able to find the Nambunians as described in [17].

$$\begin{aligned} H_1(x, y, z) &= \frac{1}{2}y^2 + \frac{1}{2}z^2 - \rho z \\ H_2(x, y, z) &= -\frac{1}{2}x^2 + \sigma z \end{aligned} \tag{17}$$

From Lemma III.2, we are able to conclude that a trajectory starting at $(x_{ND}(0), y_{ND}(0), z_{ND}(0))$ will always lie in the intersection of

$$\begin{aligned} H_1(x_{ND}(t), y_{ND}(t), z_{ND}(t)) &= H_1(x_{ND}(0), y_{ND}(0), z_{ND}(0)) \\ H_2(x_{ND}(t), y_{ND}(t), z_{ND}(t)) &= H_2(x_{ND}(0), y_{ND}(0), z_{ND}(0)) \end{aligned} \tag{18}$$

We show this occurrence in Figure 14 by taking the initial condition $(x_{ND}(0), y_{ND}(0), z_{ND}(0)) = (1, 5, -1)$ and plotting the corresponding trajectory and the surfaces defined in Equation (18).

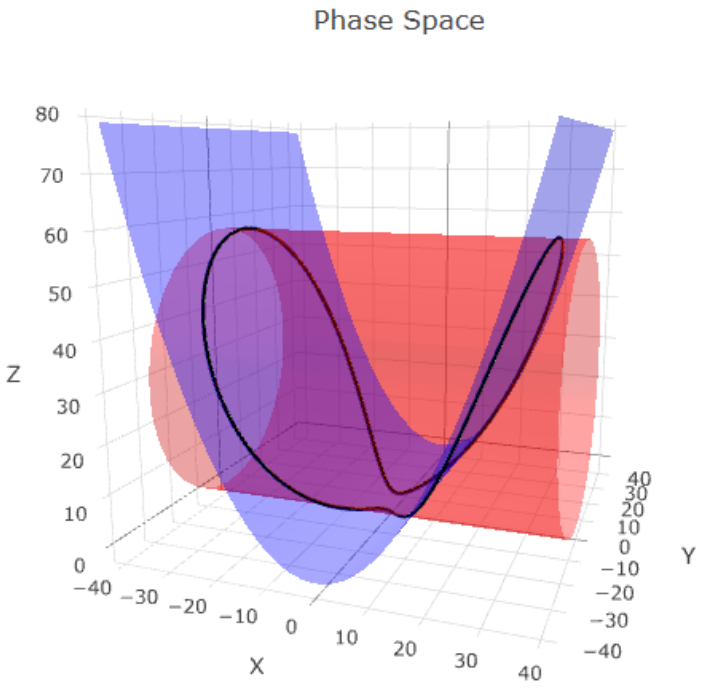

Figure 14: *The nondissipative part of the Lorenz system as the intersection between the surfaces defined in Equation* (18).

Let us now recombine the dissipative part of the Lorenz system with the nondissipative part and see what conclusions we can make. The following analysis is based off of [17], which we refer to for a more complete overview. We start by focusing on the Nambunian H_1.

ii.1 The Nambunian H_1

Because of Lemma III.2, we know that $\dot{H}_1(x_{ND}, y_{ND}, z_{ND}) = 0$. However, this is not the case for the recombined, original Lorenz system. In this case,

$$\dot{H}_1(x, y, z) = \beta z(\rho - z) - y^2$$

Notice that $\dot{H}_1(x, y, z) \leq 0$ for all points in the phase space where $y^2 + \beta(z - \rho/2)^2 \geq \beta\rho^2/4$. This is equivalent to saying that $\dot{H}_1(x, y, z) \leq 0$ for all points "outside" the cylinder $y^2 + \beta(z - \rho/2)^2 = \beta\rho^2/4$.

Say we have some trajectory $\mathbf{T}(t) = (x_\mathbf{T}(t), y_\mathbf{T}(t), z_\mathbf{T}(t))$ with initial condition

$\mathbf{T}(0) = (x_0, y_0, z_0)$. Say $\tau \in \mathbb{R}$, then

$$S_1(\mathbf{T}(0), \tau) \equiv \frac{1}{2}y^2 + \frac{1}{2}z^2 - \rho z = H_1(\mathbf{T}(\tau)) \equiv y^2 + (z-\rho)^2 = 2H_1(\mathbf{T}(\tau)) + \rho^2 \quad (19)$$

defines the surface that contains the point $\mathbf{T}(\tau)$ of our trajectory, and still contains the nondissipative solution of the Lorenz system with the initial condition $\mathbf{T}(0)$. Notice that $S_1(\mathbf{T}(0), \tau)$ describes a cylinder in the phase space.

To find some surface of a similar shape to $S_1(\mathbf{T}(0), \tau)$ that localizes the Lorenz Attractor, suppose there exists some $k > -\frac{1}{2}\rho^2$ so that $\dot{H}_1(x, y, z) < 0$ for all points in the phase space outside the cylinder

$$S_k \equiv y^2 + (z-\rho)^2 = 2k + \rho^2$$

Notice that S_k is exactly the same as $S_1(\mathbf{T}(0), \tau)$ when $H_1(\mathbf{T}(\tau)) = k$. We know such a k exists since we know from above that $\dot{H}_1(x, y, z) \leq 0$ for all points outside the cylinder $y^2 + \beta(z - \rho/2)^2 = \beta\rho^2/4$.

We can conclude that if trajectory $\mathbf{T}(t)$ has its initial condition outside of S_k, then there must exist a $\mathcal{T} \in \mathbb{R}_{>0}$ so that $\forall t < \mathcal{T}$, $\dot{H}_1(\mathbf{T}(t)) < 0$. It is to be noted that $\mathcal{T}$ is specific for each trajectory. This means that with time, $S_1(\mathbf{T}(0), t)$ will shrink in radius $\forall t < \mathcal{T}$. However, since $\mathbf{T}(t)$ is always found on $S_1(\mathbf{T}(0), t)$ per construction, this is equivalent to saying that $\mathbf{T}(t)$ will get closer and closer to some subset inside or on the cylinder S_k $\forall t < \mathcal{T}$.

Assume without loss of generality that $\dot{H}_1(\mathbf{T}(\mathcal{T})) = 0$. Then $\mathbf{T}(\mathcal{T})$ must be inside or on the cylinder S_k. However, we know then that $\mathbf{T}(t)$ cannot return back to the outside of S_k since we just saw that any trajectory with any initial condition outside of S_k must be unequivocally drawn towards S_k. Therefore, $\mathbf{T}(t)$ will stay inside or on S_k for all $t \geq \mathcal{T}$. In conclusion, we have proven that $\mathbf{T}(t)$ will be attracted to some subset of the surface or interior of S_k. Since we have not specified the trajectory $\mathbf{T}(t)$, we can conclude that all attractors, global or otherwise, are found inside or on S_k, including the Lorenz Attractor!

After a rather long-winded explanation of why S_k will contain all attractors of the Lorenz System, we can easily see that the Lorenz Attractor must be found inside the set of the phase space where

$$y^2 + (z-\rho)^2 \leq 2k + \rho^2$$

However, we now hope to find the optimal k in order to localize the Lorenz Attractor

as efficiently as possible. In essence, we wish to find

$$k_{min} = \min\{k > -\frac{1}{2}\rho^2 \mid \dot{H}_1(x,y,z) \leq 0 \quad \forall (x,y,z) \text{ where } y^2 + (z-\rho)^2 \geq 2k + \rho^2\}$$

Reference [17] redefines this value (using k_{max} instead of k_{min}) as

$$U_0 = \{(x,y,z) \in \mathbb{R}^3 \mid \dot{H}_1(x,y,z) = 0\}$$
$$k_{min} = \max\{H_1(x,y,z) \mid (x,y,z) \in U_0\}$$

What is important is that this is a constrained optimization problem that can be solved using Lagrange's Multiplier Method (see [5]). Sparing the extraneous details, we see that the Lorenz Attractor must be found somewhere in the set

$$\{(x,y,z) \in \mathbb{R}^3 \mid y^2 + (z-\rho)^2 \leq 2k_{min} + \rho^2\}$$
where
$$k_{min} = H_1\left(0, \frac{\pm\beta\rho}{2-2\beta}\sqrt{\beta-2}, \frac{\rho(2-\beta)}{2-2\beta}\right) = \frac{\rho^2(\beta-2)^2(\beta-1)}{2(2-2\beta)^2} \tag{20}$$

We show that this is indeed the case in Figure 15 by plotting the Lorenz Attractor along with boundary of the localizing set defined in Equation (20).

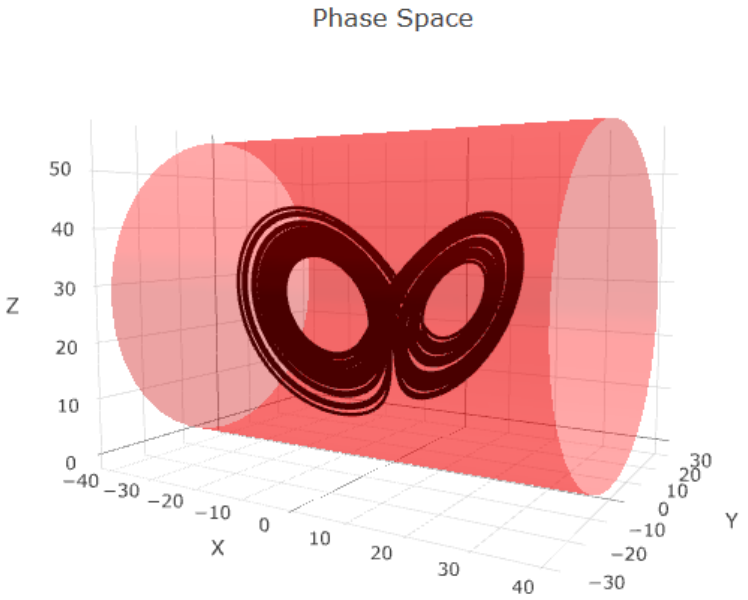

Figure 15: *The Lorenz Attractor, nestled comfortably within the localizing set defined in Equation* (20).

ii.2 The Nambunian H_2

Just as with H_1, we know that $\dot{H}_2(x_{ND}, y_{ND}, z_{ND}) = 0$. However, this is not the case for the recombined, original Lorenz system. In this case,

$$\dot{H}_2(x, y, z) = \sigma(x^2 - \beta z)$$

Notice that $\dot{H}_2(x, y, z) \geq 0$ for all points in the phase space where $x^2 \geq \beta z$. This is equivalent to saying that $\dot{H}_2(x, y, z) \geq 0$ for all points "below" the paraboloid $x^2 = \beta z$.

Say we have some trajectory $\mathbf{T}(t) = (x_{\mathbf{T}}(t), y_{\mathbf{T}}(t), z_{\mathbf{T}}(t))$ with initial condition $\mathbf{T}(0) = (x_0, y_0, z_0)$. Say $\tau \in \mathbb{R}$, then

$$S_2(\mathbf{T}(0), \tau) \equiv -\frac{1}{2}x^2 + \sigma z = H_2(\mathbf{T}(\tau)) \equiv z - \frac{H_2(\mathbf{T}(\tau))}{\sigma} = \frac{x^2}{2\sigma} \tag{21}$$

defines the surface that contains the point $\mathbf{T}(\tau)$ of our trajectory, and still contains the nondissipative solution of the Lorenz system with the initial condition $\mathbf{T}(0)$. Notice that $S_2(\mathbf{T}(0), \tau)$ describes a paraboloid in the phase space.

To find some surface of a similar shape to $S_2(\mathbf{T}(0), \tau)$ that localizes the Lorenz Attractor, suppose there exists some $k \in \mathbb{R}$ so that $\dot{H}_2(x, y, z) > 0$ for all points in the phase space "below" the paraboloid

$$S_k \equiv z - \frac{k}{\sigma} = \frac{x^2}{2\sigma}$$

Notice that S_k is exactly the same as $S_2(\mathbf{T}(0), \tau)$ when $H_2(\mathbf{T}(\tau)) = k$. We know such a k exists since we know from above that $\dot{H}_2(x, y, z) \geq 0$ for all points below the paraboloid $x^2 = \beta z$.

Similar to our analysis with the Nambunian H_1, we can conclude that if trajectory $\mathbf{T}(t)$ has its initial condition below S_k, then there must exist a $\mathcal{T} \in \mathbb{R}_{>0}$ so that $\forall t < \mathcal{T}$, $\dot{H}_2(\mathbf{T}(t)) > 0$. It is to be noted that $\mathcal{T}$ is specific for each trajectory. This means that with time, $S_2(\mathbf{T}(0), t)$ will shift upwards in the positive z-direction $\forall t < \mathcal{T}$. However, since $\mathbf{T}(t)$ is always found on $S_2(\mathbf{T}(0), t)$ per construction, this is equivalent to saying that $\mathbf{T}(t)$ will get closer and closer to some subset above or on the paraboloid S_k $\forall t < \mathcal{T}$.

Again assume without loss of generality that $\dot{H}_2(\mathbf{T}(\mathcal{T})) = 0$. Then $\mathbf{T}(\mathcal{T})$ must be above or on the paraboloid S_k. However, we know then that $\mathbf{T}(t)$ cannot return to the area underneath S_k since we just saw that any trajectory with any initial

condition underneath S_k must be unequivocally drawn towards S_k. Therefore, $\mathbf{T}(t)$ will stay above or on S_k for all $t \geq \mathcal{T}$. In conclusion, we have proven that $\mathbf{T}(t)$ will be attracted to some subset of the surface or area above S_k. Since we have not specified $\mathbf{T}(t)$, we can conclude that all attractors, global or otherwise, are found above or on S_k, including the Lorenz Attractor. Thus, we can conclude that the Lorenz Attractor must be found inside the set of the phase space where

$$z \geq \frac{x^2 + 2k}{2\sigma}$$

However, we now hope to once again find the optimal k in order to localize the Lorenz Attractor as efficiently as possible. In essence, we wish to find

$$k_{max} = \max\left\{k \in \mathbb{R} \mid \dot{H}_2(x, y, z) \geq 0 \quad \forall (x, y, z) \text{ where } z \leq \frac{x^2 + 2k}{2\sigma}\right\}$$

Reference [17] redefines this value as

$$\begin{aligned} U_0 &= \{(x, y, z) \in \mathbb{R}^3 \mid \dot{H}_2(x, y, z) = 0\} \\ k_{max} &= \max\{H_2(x, y, z) \mid (x, y, z) \in U_0\} \end{aligned}$$

Once again, this is a constrained optimization problem that can be solved using Lagrange's Multiplier Method (see [5]). Sparing the extraneous details, we see that the Lorenz Attractor must be found somewhere in the set

$$\begin{aligned} &\left\{(x, y, z) \in \mathbb{R}^3 \mid z \geq \frac{x^2 + 2k_{max}}{2\sigma}\right\} \\ &\text{where} \\ &k_{max} = H_2(0, 0, 0) = 0 \end{aligned} \tag{22}$$

We show that this is indeed the case in Figure 16 by plotting the Lorenz Attractor along with boundary of the localizing set defined in Equation (22).

As a result, we are able to localize the Lorenz Attractor using the Nambunians H_1 and H_2. We represent these results in Figure 17 by plotting the Lorenz Attractor along with boundary of the localizing sets defined in Equations (20) and (22).

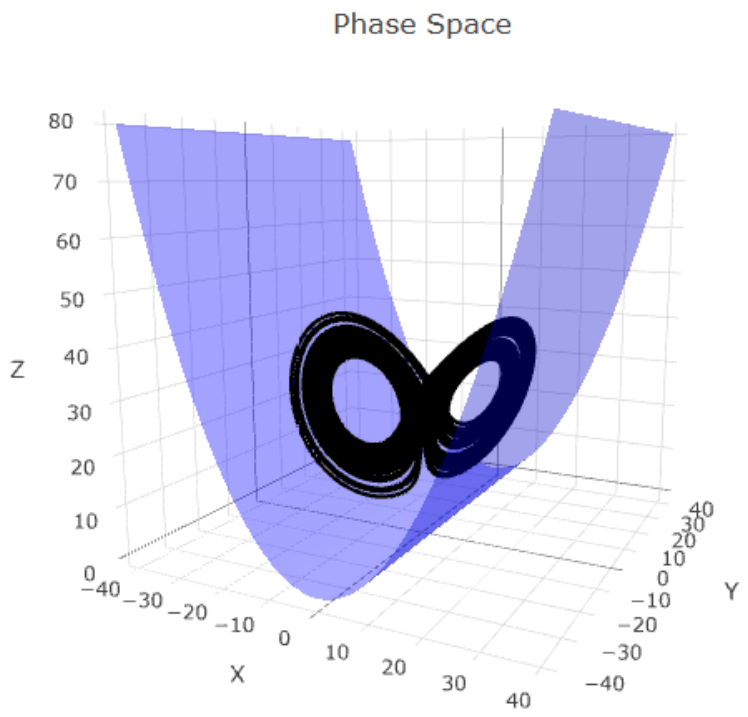

Figure 16: *The Lorenz Attractor, nestled comfortably within the localizing set defined in Equation* (22).

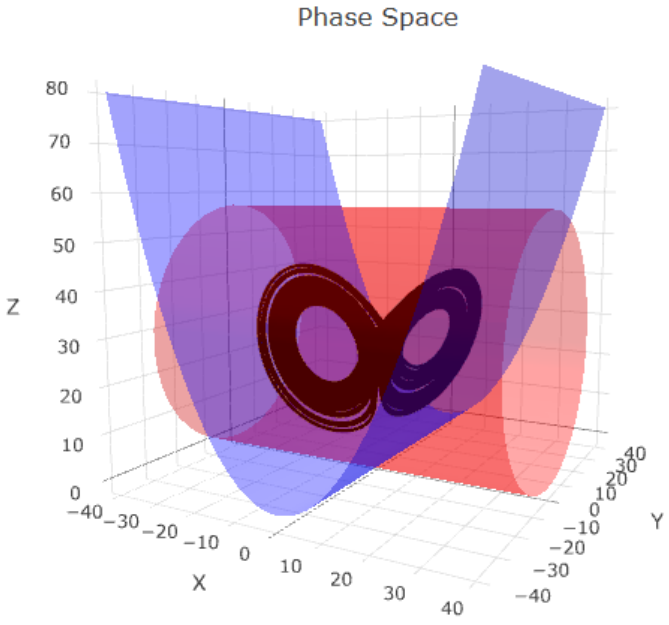

Figure 17: *The Lorenz Attractor, nestled comfortably within the localizing sets defined in Equations* (20) *and* (22).

As a concluding note, recall Lemma III.3. From this lemma, we know that we can construct an infinite number of Nambunian pairs using H_1 and H_2, and in-so-doing an infinite number of different localizing sets just like those constructed in Equations (20) and (22). Therefore, a more intensive analysis using multiple pairs of localizing sets could lead to a very efficient localization of the Lorenz Attractor indeed.

Of course, this method is only applicable to systems that have a nonzero nondissipative part, for which the Nambunians can be found (which is a difficult task in and of itself). The analysis that follows is also rather lengthy and may not even be possible. It all depends on how the Nambunians behave and interact with the system, which can make analysis difficult if not impossible. In conclusion, this method can be very efficient in localizing strange attractors, but can only be applied effectively to a limited number of dynamical systems due to the cost of finding the appropriate Nambunian functions.

IV. A Geometric Approach to Localization using Competitive Modes

We now get to the heart of this literary analysis: a preliminary analysis of a geometric approach in localizing strange attractors. For this, we will first explore a thorough understanding of the concept of competitive modes of a system of differential equations, and from this we will move on to using these competitive modes geometrically.

i. Competitive Modes

As a toy example, let us take the following differential equation for a simple oscillator.

$$\begin{cases} \dot{x} = y \\ \dot{y} = -\alpha x \text{ with } \alpha \geq 0 \end{cases}$$

This equation can be solved exactly by the equation below.

$$\begin{aligned} x(t) &= x(0)\cos\left(\sqrt{\alpha}t\right) + \frac{y(0)}{\sqrt{\alpha}}\sin\left(\sqrt{\alpha}t\right) \\ y(t) &= -x(0)\sqrt{\alpha}\sin\left(\sqrt{\alpha}t\right) + y(0)\cos(\sqrt{\alpha}t) \end{aligned}$$

What we notice is that $x(t)$ is periodic, with a frequency of $\sqrt{\alpha}/2\pi$. For this reason, we (the authors) simply call α the squared frequency of the oscillation: only $\sqrt{\alpha}$ affects the frequency of the oscillator. We will apply this concept to much more general systems.

We take a general n-dimensional autonomous system of differential equations $\dot{x}_i = F_i(\mathbf{x})$ with $i \in \{1, 2, \cdots, n\}$. We can easily transform this system into a system of interconnected oscillators as follows [4][24]:

$$\begin{aligned} \ddot{x}_i &= \dot{F}_i(\mathbf{x}) \\ &= \sum_{j=1}^{n} \frac{\partial F_i}{\partial x_j}(\mathbf{x})\frac{\partial x_j}{\partial t} \\ &= \sum_{j=1}^{n} \frac{\partial F_i}{\partial x_j}(\mathbf{x})F_j(\mathbf{x}) = f_i(\mathbf{x}) \end{aligned} \tag{23}$$

This of course only works if F_i is x_j-differentiable for all $i, j \in \{1, 2, \cdots, n\}$. However, if this is the case, we make one more assumption, which we give below [4][24].

$$f_i(\mathbf{x}) = h_i(x_1, \cdots, x_{i-1}, x_{i+1}, \cdots, x_n) - x_i g_i(x_1, \cdots, x_n) \ \forall i \in \{1, 2, \cdots, n\} \tag{24}$$

If both Equation (23) and Equation (24) hold, then we can rewrite our original system of differential equations into the form given below [4][24].

$$\begin{cases} \ddot{x}_1 + g_1(x_1, \cdots, x_n)x_1 = h_1(x_2, \cdots, x_n) \\ \ddot{x}_2 + g_2(x_1, \cdots, x_n)x_2 = h_2(x_1, x_3, \cdots, x_n) \\ \cdots \\ \ddot{x}_i + g_i(x_1, \cdots, x_n)x_i = h_i(x_1, \cdots, x_{i-1}, x_{i+1}, \cdots, x_n) \\ \cdots \\ \ddot{x}_n + g_n(x_1, \cdots, x_n)x_n = h_n(x_1, \cdots, x_{n-1}) \end{cases} \tag{25}$$

In a sense, we have turned our system into a system of interconnected, nonlinear oscillators.

Definition IV.1. ***Competitive Modes*** *Say we have the n-dimensional autonomous system of differential equations* $\dot{\mathbf{x}} = \mathbf{F}(\mathbf{x})$. *If Equation* (23) *and Equation* (24) *hold for this system, then the system can be transformed as shown in Equation* (25). *The solutions* x_i *for Equation* (25) *are then known as the competitive modes of the system, with* g_i *and* h_i *being the corresponding squared frequency functions and forcing functions, respectively [4][24].*

Currently, there is an open conjecture connecting chaos and competitive modes together, and it is presented as follows.

Conjecture IV.1. *The conditions for a dynamical system to be chaotic are given below (assuming Equation* (23) *and Equation* (24) *hold) [4][24]:*

- *there exist at least two squared frequency functions in the system;*
- *at least two squared frequency functions* g_i *and* g_j *are competitive or nearly competitive; that is, there exists* $t \in \mathbb{R}$ *so that* $g_i(t) \approx g_j(t)$ *and* $g_i(t), g_j(t) > 0$*;*
- *at least one squared frequency function is a function of evolution variables such as* t*;*
- *at least one forcing function is a function of the system variables.*

ii. An example using the classical Lorenz system

The Lorenz system as defined in Equation (4) has been used for a plethora of experiments involving chaos, and now it once again provides a useful framework to test the potentiality of Conjecture IV.1.

Using the definition of the Lorenz system, we can easily see why the following system of equations is valid.

$$\begin{cases} \ddot{x} = \sigma(\sigma + \rho - z)x - \sigma(\sigma + 1)y \\ \ddot{y} = (\sigma(\rho - z) + 1 - x^2)y + ((\beta + \sigma + 1)z - \rho(\sigma + 1))\, x \\ \ddot{z} = (\beta^2 - x^2)z + (\rho x^2 - (\beta + \sigma + 1)xy + \sigma y^2) \end{cases}$$

Decomposing this, we can then easily define the squared frequency functions

$$\begin{aligned} g_1(x, y, z) &= \sigma z - \sigma(\sigma + \rho) \\ g_2(x, y, z) &= x^2 + \sigma z - (\sigma\rho + 1) \\ g_3(x, y, z) &= x^2 - \beta^2 \end{aligned} \tag{26}$$

and the forcing term functions

$$\begin{aligned} h_1(y, z) &= -\sigma(\sigma + 1)y \\ h2(x, z) &= (\beta + \sigma + 1)xz - \rho(\sigma + 1)x \\ h3(x, y) &= \rho x^2 - (\beta + \sigma + 1)xy + \sigma y^2 \end{aligned} \tag{27}$$

We notice that

- there exist at least two squared frequency functions in the system, i.e. there are at least 2 g functions;
- at least one squared frequency function is a function of evolution variables such as t, i.e. at least one g function is not a constant;
- at least one forcing term function is a function of the system variables, i.e. at least one h function is not a constant.

All that remains is to investigate whether at least two squared frequency functions are competitive or nearly competitive. To do this, we choose the classic parameters $\sigma = 10$, $\rho = 28$, and $\beta = 8/3$ and plot a trajectory into the Lorenz Attractor, as shown in Figure 18. For every point in the trajectory, we plot the values of g_1 (in red), g_2 (in green), and g_3 (in blue), shown in Figure 19.

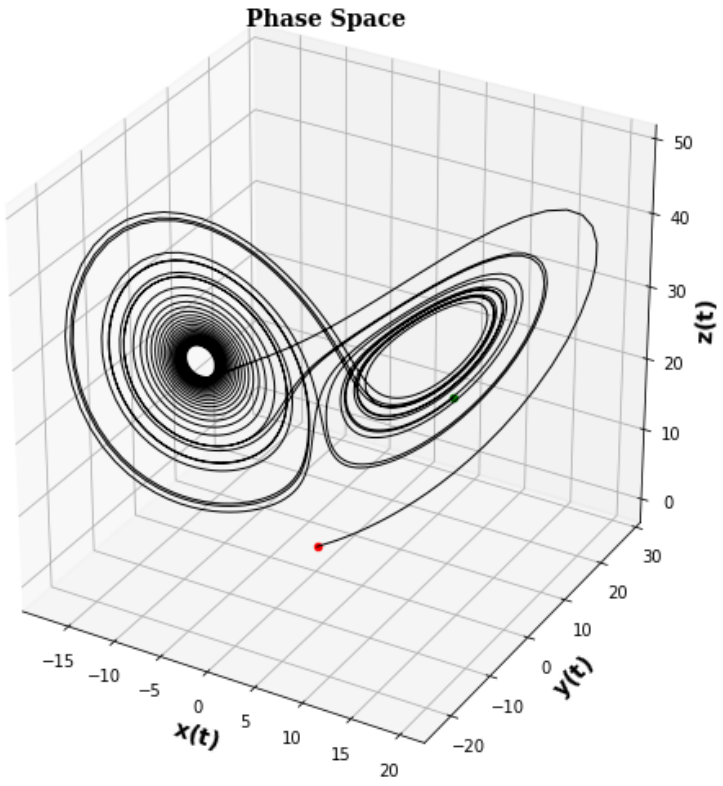

Figure 18: *A trajectory through the classical Lorenz system where* $\sigma = 10$*,* $\rho = 28$*, and* $\beta = 8/3$ *and* $x(0) = 0.1$*,* $y(0) = 0.1$*,* $z(0) = 0.1$*.*

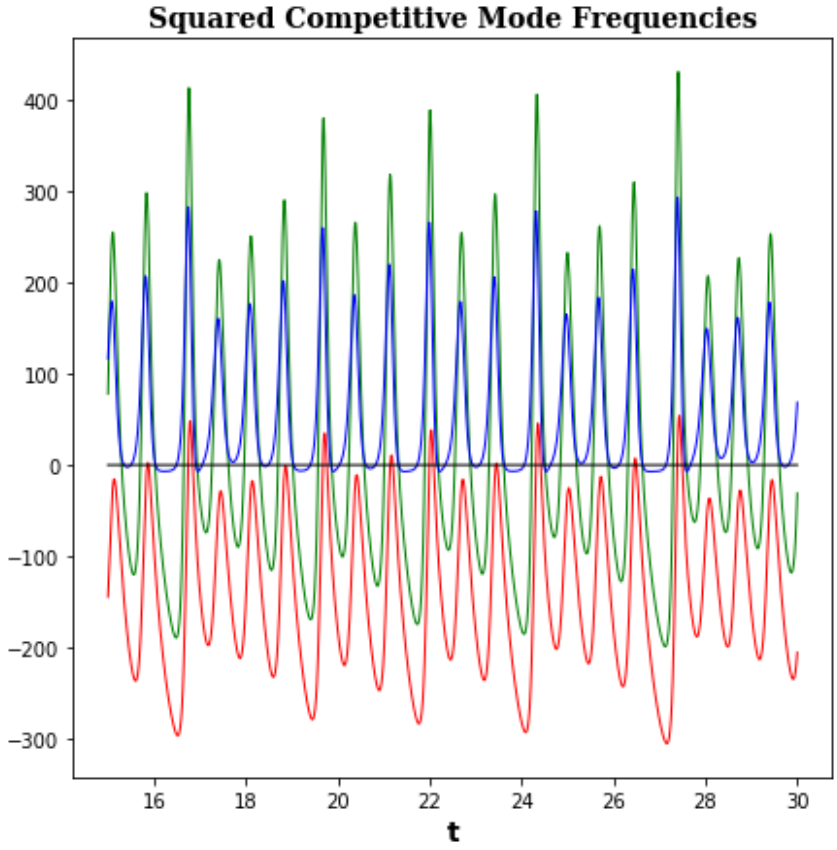

Figure 19: *The squared frequency functions g_1 (given in red), g_2 (given in green), and g_3 (given in blue) of the trajectory shown in Figure 18. We only plot for $t \geq 15$ to ensure that the trajectory in Figure 18 is inside the Lorenz Attractor.*

We notice from Figure 19 that g_1 is always less than g_2. This can be easily proven to be true. Consider the difference $g_2(x, y, z) - g_1(x, y, z) = x^2 + (\sigma^2 - 1)$. Since $\sigma > 1$, we then immediately see that $g_2(x, y, z) - g_1(x, y, z) > 0$. Thus, we only have to focus on the potential intersections between g_1 and g_3, and g_2 and g_3 [24].

Focusing our attention on g_1 and g_3, we see that
$g_3(x, y, z) - g_1(x, y, z) = x^2 - \sigma z + (\sigma(\sigma + \rho) - \beta^2)$. If $g_3 - g_1 = 0$, then we can conclude that

$$\sigma z = x^2 + \left(\sigma(\sigma + \rho) - \beta^2\right) \tag{28}$$

Investigating Figure 19, we see that g_1 is always less than g_3 while in the Lorenz Attractor. This has two results. First of all, the interaction between g_1 and g_3 can not lead to the Lorenz Attractor exhibiting chaos according to Conjecture IV.1. Second, when looking at the situation in a "reverse" point of view, we see that since

$g_3(x, y, z) > g_1(x, y, z)$ for all points $(x, y, z) \in \mathbb{R}^3$ in the Lorenz Attractor, the attractor must lie under the plane defined in Equation 28 (which is indeed the case). This phenomenon is shown in Figure 20.

Focusing our attention on g_2 and g_3, we see that
$g_2(x, y, z) - g_3(x, y, z) = \sigma z + (\beta^2 - \sigma\rho - 1)$. If $g_2 - g_3 = 0$, then we can conclude that

$$\sigma z = \sigma\rho + 1 - \beta^2 \tag{29}$$

Investigating Figure 19, we see that g_2 and g_3 do intersect regularly while in the Lorenz Attractor. This has two results. First of all, since g_2 and g_3 are competitive, Conjecture IV.1 claims that the Lorenz Attractor is chaotic (which is indeed the case). Second, when we again look at the situation in a "reverse" point of view, we see that since $g_3(x, y, z) = g_1(x, y, z)$ for some points $(x, y, z) \in \mathbb{R}^3$ in the Lorenz Attractor, the attractor must intersect the plane defined in Equation 29 (which is indeed the case). This phenomenon is shown in Figure 20.

This "reversing" of viewpoints is the key to understanding how Conjecture IV.1 can be used to localize a strange attractor in a comparatively easy way. First, one can transform (if possible) the system of differential equations in question into the form given by Equation (25). From this, the squared frequency functions $\{g_i\}$ can easily be defined. Once they are, one can define surfaces in the phase space where these squared frequency functions intersect each other. Then, if Conjecture IV.1 is true, any strange chaotic attractor must be found in a set that touches or passes through at least one of these intersection surfaces.

In conclusion, Conjecture IV.1 is valid for the Lorenz System since it accurately predicts chaos, shown by this and other similar analyses [3][4][24]. On the other hand, the conjecture is able to accurately predict the general location of the Lorenz Attractor. This method can then be applied more generally to other dynamical systems to help determine where chaotic attractors may be located.

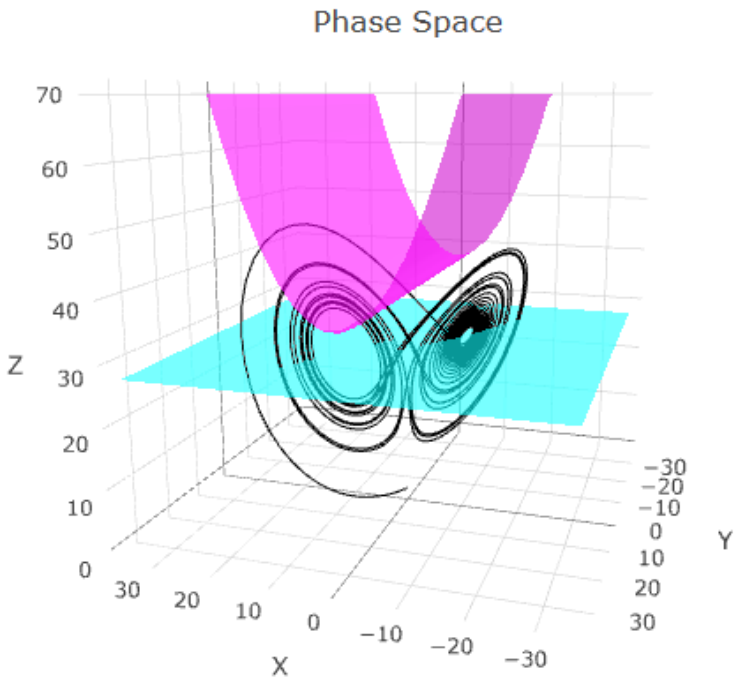

Figure 20: *The intersection surfaces defined in Equation* (28) *(given in magenta) and in Equation* (29) *(given in cyan). We see that the Lorenz Attractor is found entirely under the intersection surface defined in Equation* (28)*, and touching the intersection surface defined in Equation* (29)*.*

V. Conclusions

Strange attractors are an intriguing result from the study of dynamical systems. Though their structures are both beautiful and intricate in nature, they represent the steady-state solutions found in a dynamical system and therefore demand academic research in order to be understood as best as they can be.

Localizing a strange attractor can be the first step in learning more about these structures. Current localization algorithms, though invaluable in this field of research, can be quite costly. Most require reworking the corresponding system of differential equations into a pre-existing format, one that has been researched extensively and provides concrete results. The issue lies not in the existence of these formats, but rather in the effort and puzzling needed to coerce the dynamical system in question into one of these formats.

The new method highlighted in this document involving the localization of chaotic attractors through competitive modes, is an attempt at localizing attractors robustly and with a minimum amount of effort. Though this localization technique may be less conclusive than other methods, more research is required to understand the validity, application, and results of this method. In doing so, we can provide a clear understanding of a technique that could be very useful indeed.

As such, for this Master thesis, we focus on the following research questions.

- For which well-known dynamical systems is Conjecture IV.1 valid?
- Is Conjecture IV.1 true and can it be proven?
- Supposing that Conjecture IV.1 is true, can we use it to develop even more accurate localization techniques?
- Can Conjecture IV.1 also be applied to discrete dynamical systems?

References

[1] K. Astrom and R. Murray. *Feedback Systems: An Introduction for Scientists and Engineers*, chapter 8, pages 229–262. Princeton University Press, 2009. ISBN 978-0-691-13576-2. URL http://www.cds.caltech.edu/~murray/books/AM05/pdf/am08-complete_22Feb09.pdf.

[2] M. Cencini, F. Cecconi, and A. Vulpiani. *Chaos: From Simple Models to Complex Systems*, volume 17 of *Series on Advanced in Statistical Mechanics*. World Scientific Publishing Co. Pte. Ltd., 2009. ISBN 978-981-4277-65-5.

[3] G. Chen, P. Yu, and W. Yao. Analysis on topological properties of the lorenz and the chen attractors using gcm. *International Journal of Bifurcation and Chaos*, 17(8):2791–2796, 2007. URL https://www.worldscientific.com/doi/10.1142/S0218127407018762.

[4] S.R. Choudhury and R.A. Van Gorder. Competitive modes as reliable predictors of chaos versus hyperchaos and as geometric mappings accurately delimiting attractors. *Nonlinear Dynamics*, 69(4):2255–2267, 2012. URL https://link.springer.com/article/10.1007/s11071-012-0424-0.

[5] Harvard University-Mathematics Department. Lagrange multipliers. URL http://www.math.harvard.edu/archive/21a_spring_09/PDF/11-08-Lagrange-Multipliers.pdf.

[6] E. Doedel, B. Krauskopf, and H. Osinga. Global bifurcations of the lorenz manifold. *Nonlinearity*, 19(12):2947–2972, 2006. URL https://iopscience.iop.org/article/10.1088/0951-7715/19/12/013/meta.

[7] K. Falconer. *Fractal Geometry: Mathematical Foundations and Applications*. John Wiley & Sons Ltd, 2 edition, 2003. ISBN 978-0-470-84861-8.

[8] T. Feagin. High-order m-symmetric Runge-Kutta methods. In *Proceeding of the 23rd Biennial Conference on Numerical Analysis*, Strathclyde University, Glasgow, Scotland, June 2009. URL http://sce.uhcl.edu/rungekutta/.

[9] T. Feagin. High-order explicit Runge-Kutta methods using m-symmetry. *Neural, Parallel and Scientific Computations*, 20(4):437–458, 2012.

[10] N. Kuznetsov and G. Leonov. Hidden attractors in dynamical systems. from hidden oscillations in hilbert-kolmogorov, aizerman, and kalman problems to hidden chaotic attractors in chua's circuits. *International Journal of Bifurcation and Chaos*, 23(1), 2013. URL https://www.worldscientific.com/doi/pdf/10.1142/S0218127413300024.

[11] N. Kuznetsov and G. Leonov. Hidden attractors in dynamical systems: systems with no equilibria multistability and coexisting attractors. *19th IFAC World Congress Proceedings*, 47(3):5445–5454, 2014. URL https://www.sciencedirect.com/science/article/pii/S1474667016424614.

[12] N. Kuznetsov, O. Kuznetsova, G. Leonov, and V. Vagaitsev. Analytical-numerical localization of hidden attractors in electrical chua's circuit. *Lecture Notes in Electrical Engineering*, 174:149–158, 2013. URL https://link.springer.com/chapter/10.1007%2F978-3-642-31353-0_11.

[13] B. Mandelbrot. *Fractals: Form, Chance, and Dimension*. W. H. Freeman and Company, 1 (augmented) edition, 1977. ISBN 978-0-7167-0473-7.

[14] T. Matsumoto. A chaotic attractor from chua's circuit. *IEEE Transactions on Circuits and Systems*, 31(12):1055–1058, 1984. URL https://people.eecs.berkeley.edu/~chua/papers/Matsumoto84.pdf.

[15] Lawrence Perko. *Differential Equations and Dynamical Systems*, volume 7 of *Texts in Applied Mathematics*. Springer-Verlag New York, 3 edition, 2009. ISBN 978-0-387-95116-4.

[16] O. Rossler. An equation for continuous chaos. *Physics Letters A*, 57(5):397–398, 1976. URL https://www.sciencedirect.com/science/article/abs/pii/0375960176901018.

[17] Z. Roupas. Phase space geometry and chaotic attractors in dissipative nambu mechanics. *Journal of Physics A: Mathematical and Theoretical*, 45(19), 2012. URL https://iopscience.iop.org/article/10.1088/1751-8113/45/19/195101.

[18] Valentin Siderskiy. Chua's circuit diagrams, equations, simulations and how to build. URL http://www.chuacircuits.com/.

[19] C. Sparrow. An introduction to the lorenz equations. *IEEE Transactions on Circuits and Systems*, 30(8):533–542, 1983. URL https://ieeexplore.ieee.org/document/1085400.

[20] L. Takhtajan. On foundation of the generalized nambu mechanics. *Communications in Mathmatical Physics*, 160(2):295–315, 1994. URL https://link.springer.com/article/10.1007/BF02103278.

[21] R. Taylor. Attractors: Nonstrange to chaotic. *Society for Industrial and Applied Mathematics*, 2011. URL https://www.researchgate.net/publication/275400091_Attractors_Nonstrange_to_Chaotic/references.

[22] W. Tucker. A rigorous ode solver and smale's 14th problem. *Foundations of Computational Mathematics*, 2(1):53–117, 2002. URL `http://www2.math.uu.se/~warwick/main/rodes.html`.

[23] Ferdinand Verhulst. *Nonlinear Differential Equations and Dynamical Systems*. Universitext. Springer-Verlag Berlin Heidelberg, 2 edition, 2000. ISBN 978-3-540-60934-6.

[24] P. Yu. *Edited Series on Advances in Nonlinear Science and Complexity*, volume 1, chapter 1, pages 1–125. Elsevier B.V., 2006. URL `https://www.sciencedirect.com/science/article/pii/S157469090601001X`.